

AN ABSTRACT OF THE THESIS OF

John David Pembrook for the Master of Science in Meteorology
(Name) (Degree) (Major)

Date thesis is presented 13 May 1964

Title OBTAINING OPTIMUM PHOTOGRAPHIC RECORDING OF
DATA FROM WEATHER RADAR PRESENTATIONS

Redacted for Privacy

Abstract approved _____
✓ (Major professor)

This paper discusses the theoretical design parameters of photographic data recording systems associated with atmospheric research radar. Practical considerations modify these theoretical results. The design of a recording system employed on the Range Height Indicator (RHI) scope of the weather Radar Set AN/CPS-9 atop McCulloch Peak, Oregon, illustrates the optimization of these modified parameters.

Finances, an ever present practical consideration, required the use of a 16 mm camera as an element of this data recording system. Calculations show this equipment, using readily available present day films, incapable of recording all the information the RHI scope presents on all radar operational modes (range and pulse length combinations). However this system satisfactorily operates on short pulse up to 50 miles range or long pulse at all ranges.

Comparable recordings of data require a constant radar returned signal strength versus scope intensity. Two methods of maintaining this relationship include: 1) measuring the parameters which control the scope intensity and 2) measuring directly the light output of the scope. Measuring directly the light output of the scope offers the more accurate and practical method. The advantages of smaller physical size and greater sensitivity favor the photoconductor as a light measuring device for use in measuring the scope intensity. A cathode ray tube (CRT) Photometer illustrates the employment of a photoconductor as the light sensing element. The CRT Photometer, measuring the scope intensity directly, senses a standard strength radar signal which a radar signal generator test set, or a prominent area of ground clutter, provides. This provides the radar operator the necessary information to maintain a constant scope intensity-echo strength relationship. The photographic system records this as a constant scope intensity-film exposure density relationship allowing accurate repeatable weather radar scope data recording.

OBTAINING OPTIMUM PHOTOGRAPHIC RECORDING OF DATA
FROM WEATHER RADAR PRESENTATIONS

by

JOHN DAVID PEMBROOK

A THESIS

submitted to

OREGON STATE UNIVERSITY

in partial fulfillment of
the requirements for the
degree of

MASTER OF SCIENCE

June 1964

APPROVED:

Redacted for Privacy

Associate Professor of Physics

In Charge of Major

Redacted for Privacy

Chairman of Department of Physics

Redacted for Privacy

Dean of Graduate School

Date thesis is presented 13 May 1964

Typed by Penny A. Self

ACKNOWLEDGEMENT

The assistance and encouragement of many dedicated Oregon State University personnel made possible the work presented in this paper. In recognition, the author sincerely wishes to thank Dr. Fred W. Decker for guidance and for providing the opportunity and the facilities for this work; John C. Garman for consultation on photographic theory and practice, and for the use of darkroom facilities; Dr. James J. Brady for consultation on the photoelectric and semiconductor phenomena; Dr. Tor Bergeron for enlightening discussions on weather radar data acquisition and storage from a research synoptic meteorologist's viewpoint; Richard W. Couch for consultation on semiconductor theory and design criteria; Kenneth H. Shreeve for technical and constructional assistance; John R. Kellogg for constructional assistance; Mrs. Carol M. Couch for typing assistance and for brewing many pots of coffee; Mrs. H. Patricia Pembroke, my wife, for encouragement, editorial, drafting, and typing assistance; and all the members of the Atmospheric Science Branch of the Science Research Institute, Oregon State University, for many helpful discussions and for providing a stimulating work atmosphere.

TABLE OF CONTENTS

	Page
INTRODUCTION	1
THE PHOTOGRAPHIC SYSTEM	4
EQUIPMENT	7
CAMERA LENS RESOLUTION	8
RADAR SYSTEM RESOLUTION	15
FILM RESOLUTION AND CHOICE	22
THE CATHODE RAY TUBE	25
PHOTOCELLS	35
Vacuum phototube	37
Photovoltaic cell	38
Photoconductor cell	39
CRT PHOTOMETER	43
SUMMARY EXAMPLE	45
CONCLUSIONS	47
SUGGESTIONS FOR FUTURE RESEARCH	49
GLOSSARY	50
BIBLIOGRAPHY	52
APPENDICES	
APPENDIX I. BEZEL CONSIDERATIONS	55
APPENDIX II. THE CRT PHOTOMETER	65
APPENDIX III. VISIBILITY CHARACTERISTIC OF THE HUMAN EYE	67
APPENDIX IV. SPECTRAL ENERGY EMISSION CHARACTERISTICS OF PHOSPHORS	68
APPENDIX V. CHARACTERISTICS OF PHOTOCELLS .	70
Spectral Absorbtion Characteristics of Photocells	70
Temperature Characteristics of Photocells	75
CRT Photometer readings versus Temperature ..	81
Clairex Photocell conductance	82

LIST OF FIGURES

Figure		Page
1	Typical Electrostatic Cathode Ray Tube Diagram	27
2	RHI Scope and Bezel Assembly, Radar Set AN/CPS-9 .	61
3	PPI Scope and Bezel Assembly, Radar Set AN/CPS-9 .	62
4	RHI Scope and Bezel Assembly, SO-12N Radar Set	63
5	CRT Photometer	64
6	CRT Photometer Circuit Diagram	65
7	Proposed Improved CRT Photometer Circuit Diagram .	66
8	Visibility Characteristic of the Human Eye	67
9	Spectral-energy Emission Characteristics of the RCA Phosphor P-5	68
10	Spectral-energy Emission Characteristics of the RCA Phosphor P-7	69
11	Spectral-energy Emission Charactersitics of the RCA Phosphor P-11	69
12	Clairex Type 2 Photoconductor Cell Cadmium Sulfide .	70
13	Clairex Type 3 Photoconductor Cell Cadmium Selenide	70
14	Clairex Type 4 Photoconductor Cell Cadmium Selenide	71
15	Clairex Type 5 Photoconductor Cell Cadmium Sulfide .	71
16	Clairex Type 7 Photoconductor Cell Cadmium Sulfide .	72
17	RCA S-12 Photoconductor Cell	72
18	RCA S-14 Photoconductor Cell	73
19	RCA S-15 Photoconductor Cell	73
20	RCA Photovoltaic Cell Spectral Absorbtion Character- istics For Cell Types SL 2205 and SL 2206	74
21	Clairex Type 2 Photoconductor Cell Cadmium Sulfide .	75

LIST OF FIGURES (Continued)

Figure		Page
22	Clairex Type 3 Photoconductor Cell Cadmium Selenide	76
23	Clairex Type 4 Photoconductor Cell Cadmium Selenide	77
24	Clairex Type 5 Photoconductor Cell Cadmium Sulfide .	78
25	Clairex Type 7 Photoconductor Cell Cadmium Sulfide .	79
26	Typical Temperature Characteristics of an RCA Cadmium Sulfide Photoconductor Cell	80
27	CRT Photometer Readings versus Temperature	81
28	Clairex Photocell Conductance	82

OBTAINING OPTIMUM PHOTOGRAPHIC RECORDING OF DATA FROM WEATHER RADAR PRESENTATIONS

INTRODUCTION

Over the past two decades, radar technology has provided ever increasingly useful tools for the meteorologist. Weather radar provides information about the distribution of clouds and associated precipitation patterns arising out of squall lines(6), frontal movements and air mass convergence (29), modification processes (1), and orographic influences (22). The radar observes chaff drift (1, 14) and cloud shear (1), from which data the researcher may analyze the wind structure of the atmosphere.

The radar system as a tool consists essentially of a transmitter and receiver of microwave energy, and a data signal analysis and display system. The transmitter furnishes the electromagnetic wave with which the radar senses, while the receiver collects the reflected wave energy and, after amplification, gives it to the data display system. A video amplifier and cathode ray tube display system convert the long wave-length energy (1×10^8 - 20×10^8 angstrom units) which the radar employs to light energy in the visible spectrum (4300-7000 angstrom units). Thus, a human observer may view the same intelligence that the receiver views. The observer may study atmospheric processes occurring hundreds of miles away by extending his visual capabilities with radar.

The forecasting meteorologist, with only the above described radar system, may observe the formation of squall lines, the

movement of weather systems, and may quickly predict their future position by extrapolation of their current movement (1). Thus radar serves as a valuable tool to the forecasting meteorologist in this capacity. In regions where few ground observer sites exist, as over the ocean, radar proves especially useful for meteorological data collection.

Radar may serve an even more important function to the research meteorologist interested in the phenomena of the atmospheric processes producing weather which the forecaster so diligently tracks. The scope persistence, the life span of the display of information on the cathode ray tube, usually lasts only a few seconds. The researcher must have some type of permanent record of the information that the radar system displays to compare with information that observers accrue using different methods of recording the same atmospheric parameters.

Three methods for making this permanent record include:

1. Sketching the cathode ray tube display on some type of plastic overlay;
2. Recording it on video tape;
3. Photographing the display.

The third method provides a permanent and economical data storage system: a sketch does not record all the information seen and displayed by the radar system; video tape does not produce a static image unless the system employs very long persistence storage type picture tubes. Time lapse photography can produce an inexpensive high-quality static image of the display for detailed

analysis by the researchers.

This paper deals with the problems of transferring all the information displayed by the cathode ray tube radar display system to a permanent photographic record.

THE PHOTOGRAPHIC SYSTEM

A polaroid camera provides the most practical method of recording the scope display when the nature of the study requires only a partial record, as when tracking a moving storm system (16). This method allows the immediate study and dissemination of the scope record.

The serious researcher often needs a continuous record of the happenings which the radar observes, not just segments of the occurrence recorded at too-distant intervals. Hence, radar scope photography for research purposes usually means time-lapse photography, with picture frames exposed continuously as the radar probes the birth, life, and death of a weather process as these occur. After the researcher collects a complete record on film of everything the radar scope displayed, he then may study the data at length, attempting to correlate these new data with existing theorems and possibly developing new theorems from empirical relationships.

Fundamentally, the photographic data recording system consists of a time lapse movie camera mounted so it may photograph the radar scope and the bezel data (Appendix I). The modified camera shutter remains open except when the film advances between frames. The camera records a complete sweep or a multiple of sweeps on one frame, the shutter then trips, thereby advancing the film with the shutter closed to prevent blur, and the recording sequence starts over. The camera records the bezel along with the scope picture, providing the required information for frame

identification.

The requirements for a reliable photographic data recording system include:

1. A camera lens and film of sufficiently high resolution to record the limits of resolution of the cathode ray tube.
2. A method of automatically tripping the camera to free the operator for more important observational duties.
3. A bezel which displays automatically all the pertinent information, such as time, date, radar receiver gain control setting, elevation, azimuth, and other data needed for analysis of the photographic record (Appendix 1). Thus, a bezel may eliminate the chance of losing a written log of this information, or of never making a log in the first place.
4. Detailed film analysis requires a method of maintaining a constant ratio of the power returned to the radar to the intensity shown on the cathode ray tube.

Application of theoretical considerations to these requirements may produce a reliable photographic weather radar data collection system. Sample film records (Appendix I, Figures 2, 3, 4) exemplify the possibilities of such a system.

The next section deals with the problems encountered in meeting each requirement, the different suggested solutions, and the best solution which this study determined. Hopefully, others needing this type of data collection system will apply these principles to achieve their goals with a minimum of false starts, resulting in a saving of time and expense by the future weather radar

researcher. These principles also may suggest ways to modify equipment currently unsatisfactory for weather radar research purposes.

EQUIPMENT

The Range Height Indicator (RHI) scope of the weather Radar Set AN/CPS-9 stationed at McCulloch Peak, Oregon, served as the test instrument for the study.

A Model 20 Bell & Howell 16 millimeter camera with modified shutter and 20 millimeter $f/1.9$ lens, belonging to Atmospheric Science Branch, served as the basic instrument for the data recording unit.

A series of film trials determined 18 inches (457.2 millimeters) as the optimum distance from the scope to the central lens plane of the camera. At this distance, the picture area included only the bezel and radar scope. A diaphragm setting of $f/8$ gave adequate depth of field to produce a sharp image of both radar scope and bezel assembly. (See Appendix I)

A report on the theoretical check of the system follows.

CAMERA LENS RESOLUTION

The Fraunhofer diffraction theory for the limit of resolution of optical instruments gives the theoretical resolution capability of a lens (27). This paper presents only the final result of the theory since its rigid mathematical derivation serves no useful purpose here. The researcher can apply this formula in setting up an optical system--film--scope relationship for radar scope photography.

When light from a point source at infinity passes through a circular aperture, the aperture produces a Fraunhofer diffraction pattern in the image plane consisting of a circular disc surrounded by a series of dark and bright rings decreasing rapidly in intensity as their radii increase. In this manner the iris diaphragm in the camera lens produces a variable aperture which affects resolution.

As viewed from a point in the center of the lens aperture, the radius of the first ring subtends an angle Θ :

$$1) \quad \sin \Theta = 1.22 \lambda / a \quad (27)$$

λ = the wavelength of light passing through the lens

a = the aperture diameter of the lens

Now for a small angle Θ , the radius, \underline{R} , of the inner disc at the image plane approximates or equals:

$$2) \quad R = 1.22 s' \frac{\lambda}{a} \quad (27)$$

Where s' = the distance from the effective central plane of the lens to the film.

In a typical multi-element camera lens, the position of the effective central lens plane used for computation of magnification, focal planes and resolving power, usually closely approximates the position of the iris diaphragm (23).

Rayleigh (27) established an arbitrary criterion which serves as a practical guide for the researcher. It stipulates that a lens can resolve two point sources if a distance greater than their radii separates the centers of the two diffraction discs of radius R on the image plane. Hence, the angle Θ subtends, for practical purposes, the minimum angle of resolution of the lens.

Equation 2) gives the theoretical resolution capabilities of a lens which has no spherical or chromatic aberrations. Actually, all camera lenses have spherical and/or chromatic aberrations to some varying degree depending upon the lens design. In general, most camera lenses produce their sharpest image at an aperture two f/stops smaller than the largest aperture of the lens (35). Sometimes, the manufacturer will provide information concerning the resolution capabilities of a given lens. As the aperture decreases beyond design optimum, the diffraction phenomenon decreases the resolution, and as the aperture increases, spherical and/or chromatic aberrations decrease the resolution. Equation 2) gives an approximation of the resolving capabilities of a good quality lens at small aperture settings. Large apertures tend to produce the more prominent spherical and chromatic aberrations (3).

The cathode ray tube usually has a curved face, and in some systems, the bezel lies in a different plane from the scope face.

These facts often necessitate setting the camera lens at some aperture smaller than optimum in order to have all the information sharp. The above equations, 1) and 2), yield a good approximation of the decrease in resolving power with decreasing aperture.

Although the cathode ray tube cannot present a point source, the system should record the smallest image which it does present. The resolution capabilities of the lens and the resolution of the film used in the camera both affect the resulting image resolution of the system. Film manufacturers usually will provide information on the resolution capabilities of given films. The selection of a film which will resolve whatever image the lens resolves then may follow.

The above theory, applied to the Radar Set AN/CPS-9 Range Height Indicator assembly with 20 mm lens at f/8 with \underline{s} equal to 457.2 mm, showed the following theoretical maximum resolution capabilities:

$$3) \quad R = 1.22 s' \frac{\lambda}{a}$$

$$4) \quad \frac{1}{s'} = \frac{1}{f} - \frac{1}{s} \quad (27)$$

Where

f = the focal length of the lens.

s = the distance from the object to the central lens plane.

s' = the distance from the image to the central lens plane.

Then with $\underline{f} = 20$ mm and $\underline{s} = 457.2$ mm:

$$\frac{1}{s'} = \frac{1}{20 \text{ mm}} - \frac{1}{457.2 \text{ mm}}$$

$$s' = 20.915 \text{ mm}$$

and $\lambda = 7 \times 10^{-4} \text{ mm}$; (7000 angstrom units); long wavelength cut-off emitted by a P-7 phosphor used in the Radar Set AN/CPS-9 (see phosphor spectral emission curves, appendix IV).

$$5) \quad f/\text{stop} = \frac{f}{d}$$

$$d = a = \frac{f}{8} = \frac{20 \text{ mm}}{8} = 2.5 \text{ mm}$$

$$R = \frac{(1.22)(20.915 \text{ mm})(7 \times 10^{-4} \text{ mm})}{2.5 \text{ mm}}$$

$$R = 0.007146 \text{ mm}$$

$$\frac{1}{R} = 139.9 \text{ lines/mm}$$

Appendix IV shows that the P-7 phosphor has peak radiant energy wavelengths of 4350 angstroms and 5550 angstroms with the relative radiant energies as shown below.

TABLE 1. RELATIVE RADIANT ENERGIES COMPARED TO P-1 PHOSPHOR.

Relative radiant energies	Peak radiant energy wavelengths for P-7 phosphor	
	4350 Å	5550 Å
Peak	206	58
Total	272	131
Visual	16	121

Table 2 shows that filtering out the longer wavelengths and using only those of the blue phosphor produces a resolution increase of 85.4 lines per mm. However, filtering out the longer

wavelengths decreases the overall intensity of the light which contributes to the exposure of the film. This decrease in overall light energy then requires an increase in the scope intensity setting in order to achieve the original amount of film exposure and corresponding film density produced when using all the light emitted by the scope. As the scope intensity increases, an over-abundance of electrons strikes the scope phosphor, increasing halation, which decreases the resolution of the image itself.

TABLE 2. THE RESOLUTION CAPABILITIES OF A 20 MM FOCAL LENGTH LENS AT f/8 FOCUSED AT 18 INCHES, USED WITH A P-7 PHOSPHOR.

Wavelength in angstroms	Resolution (1/R) in lines per mm	R in mm
7000 Å	139.9	0.007146
5550 Å	176.5	0.005665
4350 Å	225.3	0.004439
4950 Å (λ̄)	197.9	0.005052

The lens magnification (\underline{M}) relates the scope resolution (\underline{O}) to the resolution required of the film:

The magnification of a given lens:

$$6) \quad M = \frac{s'}{s} \quad (27)$$

(3)

s' = the distance from the central plane of the lens to the image.

s = the distance from the central plane of the lens to the subject.

Designate \underline{R}^* as the radius of the smallest dot shown on a given cathode ray tube by the radar receiver as the resolving power of the cathode ray tube. Then for the camera lens to resolve \underline{R}^* , \underline{MR}^* must equal or exceed \underline{R} . For the film to record and resolve this image \underline{R} , its resolving capabilities, \underline{r} , must equal or exceed $1/\underline{R}$, with \underline{R} in millimeters and \underline{r} in lines per mm.

Applying this to the example:

$$\begin{aligned}
 7) \quad M &= \frac{s'}{s} \\
 s' &= 20.915 \text{ mm} \\
 s &= 457.2 \text{ mm} \\
 M &= 0.0457
 \end{aligned}$$

8) Since (image size) = (object size) \times M;

$$R = OM \quad (3)$$

Using the lens resolution value $\underline{R} = 0.007146$ mm, and \underline{O} = the diameter on the scope of the smallest dot the lens system resolves:

$$\begin{aligned}
 9) \quad O &= \frac{R}{M} = \frac{0.007146 \text{ mm}}{0.0457} \\
 O &= 0.1564 \text{ mm}
 \end{aligned}$$

TABLE 3. FILM RESOLUTION REQUIREMENTS AND LENS RESOLUTION CAPABILITIES AT DIFFERENT WAVELENGTHS FOR A 20 MM - f/8 - 0.0457 MAGNIFICATION LENS SYSTEM.

Scope emission wavelength λ	Lens resolution R	Resolved on scope O	Required film resolution $1/R = r$
7000 Å	0.007146 mm	0.1564 mm	139.9 lines/mm
5550 Å	0.005665 mm	0.1239 mm	176.52 lines/mm
4950 Å	0.005052 mm	0.1105 mm	197.94 lines/mm
4350 Å	0.004439 mm	0.0971 mm	225.28 lines/mm

RADAR SYSTEM RESOLUTION

The maximum resolution of the radar system as shown on the cathode ray tube limits the minimum acceptable qualities in the lens system. Assuming that the scope will resolve everything the radar receiver system will resolve, then the radar receiver-transmitter system itself serves as the limiting factor for the size image the lens system must resolve.

The pulse length and the beam width limit the transmitter resolution (1). The bandpass, the scope sweep length, and the scope sweep time limit the resolution of the receiver (11, 20). This discussion, based on the assumption that the scope resolves all that the radar receiver resolves, treats the data display system and the receiver as one continuous unit.

The receiver normally will pass only the shortest returned pulse which the radar transmits (32). Any increase over the necessary bandpass will allow the receiver to pass more noise, thereby decreasing the signal-to-noise ratio.

The resolution of the receiver system is directly proportional to the bandwidth (11, 20).

Since long range settings display more information than short range settings on a given scope area, the resolution required of the scope has a directly proportional relationship to the range setting and an inversely proportional relationship to the scope sweep length.

One half the pulse length limits the resolution of the radar system by the transmitter (1). Hence, an inversely proportional relationship exists between the required resolution of the scope and one half the pulse length.

The following equations then express the system resolution as the scope displays it:

$$10) \quad R^* = \frac{B r^* K}{L}$$

$$11) \quad R^* = \frac{r^* K'}{h L}$$

Where:

R^* = the system resolution displayed on the scope in lines/mm along the sweep line.

B = the receiver bandwidth in megacycles (mc)

r^* = the range setting in statute miles (st. mi.)

L = the scope sweep length in millimeters

h = the pulse length in microseconds

K = conversion factor constant $\frac{5.3765 \text{ lines}}{\text{mc-st. mi.}}$

K' = conversion factor constant

$\frac{10.753 \text{ lines-microsecond}}{\text{st. mi.}}$

Table 4 gives the best possible system resolutions for the Range Height Indicator scope on the Radar Set AN/CPS-9,

In the tabulation,

$R' = 1/R^*$ = diameter of the smallest dot at a given range setting and pulse length or bandpass.

Since the sweep length varies on the range height indicator scope, the setting \underline{L} equals 150 mm, the shortest sweep length. Hence it yields the largest required value of $\underline{R^*}$ for any given set of the remaining parameters. A sample calculation shows the agreement between the two equations:

When:

$$r^* = 10 \text{ st. mi.}$$

$$L = 150 \text{ mm}$$

$$B = 5.0 \text{ mc}$$

$$h = 0.5 \text{ microseconds}$$

Then:

$$R^* = \frac{Br^*K}{L} = \frac{(5 \text{ mc})(10 \text{ st. mi.})(5.3765 \text{ lines})}{(150 \text{ mm})(\text{mc-st. mi.})}$$

$$R^* = 1.7922 \text{ lines/mm}$$

$$R^* = \frac{r^*K'}{hL} = \frac{(10 \text{ st. mi.})(10.753 \text{ lines-microsecond})}{(0.5 \text{ microseconds})(150 \text{ mm})(\text{st. mi.})}$$

$$R^* = 1.4337 \text{ lines/mm}$$

The AN/TPS-10D weather radar set uses a four megacycle bandpass which just barely passes a 0.5 microsecond pulse length (32). Either equation 10) or 11) above for calculation or resolution yields identical results. As noted, the two equations produce a discrepancy in results for the Radar Set AN/CPS-9, which uses a five megacycle bandwidth to pass a 0.5 microsecond pulse (34). The bandpass equation for required scope resolution gives correct results only for radar sets designed such that the Intermediate Frequency amplifier will pass just the pulse length which the radar

transmits. This normally holds true, since any increase in bandwidth over that required to pass just the transmitted signal allows the radar to receive that much extra electronic noise, thus decreasing the signal-to-noise ratio, and in turn, decreasing the sensitivity of the radar receiver. In all radar sets, however, the Intermediate Frequency amplifier will pass the transmitted pulse length. Hence, in calculating required scope resolution, equation 11) using pulse length yields more certain results than equation 10) using bandpass. The author could not ascertain the reason for the extra bandpass built into the Radar Set AN/CPS-9 receiver.

TABLE 4. MAXIMUM RESOLUTION REQUIRED BY THE RHI SCOPE ON THE RADAR SET AN/CPS-9 USING THE EQUATION:
 $R^* = K/h L$

B = 5 mc; h = 0.5 microsecond			B = 0.5 mc; h = 5.0 microsecond	
r* st. mi.	R* lines/mm	1/R*mm	R* lines/mm	1/R* mm
10	1.434	0.6974	0.1434	6.974
25	3.585	0.2789	0.3585	2.789
50	7.170	0.1394	0.7170	1.394
75	10.755	0.0930	1.0755	0.930
100	---	---	1.434	0.6974

Table 4 shows that the RHI scope requires a higher resolution at longer ranges than at shorter ranges. The system displays more data in the same area on the scope for longer ranges than for shorter ones; hence operational procedures should require the use of the shortest range setting possible, thereby spreading the data over a

larger area of the scope face for study. The scope must resolve 10.775 lines per mm in order to show all the data that the system resolves and presents to the scope for display. The phosphor scattering of light and the halation between the scope face and the phosphor make it unlikely that the scope could resolve 10.775 lines per mm. Minimum halation and scattering occur when the scope operates at the lowest possible intensity which still records the image on the film. With these considerations, a scope resolution of 7 lines per mm at the 50 mile range and short pulse setting probably constitutes a more reasonable value in practice.

Equation 2) gives the optimum theoretical value of the lens resolution. If any doubt arises about the lens quality, assume that the scope actually resolves all that the receiver presents to it. Then the decrease in possible resolution of the scope by halation and scattering partially compensates for the decrease in the resolving power of the lens, from that theoretically determined, due to spherical and chromatic aberrations remaining in the lens. However, a good quality lens system may closely approach its theoretical resolving power capabilities.

Comparison of Table 3 with Table 4 gives the following relationships.

At the longest wavelength which the scope emits, the lens system resolves all the information presented to the scope on short pulse and 25 mile range. On short pulse and 50 mile range, it resolves 87.5% of the information. The tables also show that the lens system will resolve all the information presented to the scope

at any range on long pulse at the longest wavelength the scope will emit. The above discussion applies to the longest wavelength the scope will emit. The P-7 phosphor curve (Appendix IV) shows the longest wavelength necessary to consider for practical photography as 5550 angstroms, the highest peak response. At this wavelength, the lens system resolves everything presented to the scope on short pulse at 50 mile range. The above lens system then proves adequate if in the majority of cases the Radar Set AN/CPS-9 operates either on long pulse at any range or on short pulse at ranges of 50 miles or less. Since the mode of operation of the Radar Set AN/CPS-9 used as an example in this study fits this criterion, the author adapted the above lens system for general use on the Range Height Indicator assembly.

If the program necessitates the resolution of all the information presented to the scope at the 75 mile short pulse range setting, one may take either of two corrective measures:

- 1) Place a violet filter in front of the lens which will pass wavelengths no longer than the 4350 angstrom peak emission frequency of the blue portion of the P-7 phosphor. This alone will record a scope resolution of 10.299 lines per mm at $f/8$ (equations 3) and 9). This corresponds to 95.8% of the 10.755 lines per mm theoretically presented to the scope for display, and at the same time, it eliminates any chromatic aberration of the lens (23). But this method requires a large increase in scope intensity, to make up for the light which the filter absorbs, which produces increased scope halation and decreased scope resolution.

2) Change the f/stop of the lens to $f/4.026$ (equations 3) and 9), which resolves the 10.755 lines per mm theoretically presented to the scope at the 7000 angstrom cut-off frequency of the scope, but thus reduces depth of field.

If the program necessitates the lens actually resolving 10.755 lines per mm at the scope surface, a compromise of these two alternatives probably would achieve both the required resolution and the required depth of field. For example, use a filter which cuts off at 4350 angstroms with the 20 mm lens focused at 18 inches and set at $f/7.9964$. For practical purposes, this approximates a blue filter with the lens set at $f/8$.

FILM RESOLUTION AND CHOICE

After determining a resolution, select a film which will resolve the information which the camera lens system presents.

An explanation of the determination of film resolving power proves useful at this point:

In the measurement of resolving power for films, photographing a parallel line test chart having line and space widths of equal dimensions at a reduced scale using an optical system having at least three times the resolving capabilities of the upper limit expected of the film (7, 8, 12) gives the published values. The number of lines per millimeter just recognizable as separate lines on the film image when examined with a microscope constitutes the film resolving power (4, 12). Lines closer together than the number given as the resolving power appear as a grey mass rather than as distinguishable lines. Since the degree of development has a small effect on film resolution (21), the manufacturers validate their published film resolution values only for their recommended processing methods. Both overexposure and underexposure greatly affect the resolution capabilities of a film (7, 8, 21). The published figures on resolving power assume film exposure which produces a density range from 0.7 to 2.0 on the log density scale (7, 8). The resolving power of a film increases rapidly with an increase in image contrast of the test chart until it reaches a luminance range of about 1000/1 (7, 8). A test chart with a luminance contrast range of at least 1000/1 between the black and white lines on the chart

yields the published film resolution figures. In general, photographic film resolution improves when the film exposure light wavelengths approach the lower region of the visible spectrum (blue, violet) than in the upper (red) region (21). Due to variations in film manufacture, film processing, and resolution measurement, film manufacturers do not give specific resolution figures for given materials, but instead give a resolution range into which the film should fall.

TABLE 5. PUBLISHED RESOLVING POWERS OF A FEW READILY AVAILABLE FILMS (7, 8).

Sizes Available	Film Type	Resolving Power	ASA Film Speed
16 & 35 mm	Kodak Plus-X Pan	96 to 135 lines/mm	ASA 160/5.5 deg
35 mm	Kodak Panatomic-X Pan	136 to 225 lines/mm	ASA 40/3.5 deg
16 & 35 mm	Kodak Tri-X Pan	69 to 95 lines/mm	ASA 400/7 deg
35 mm	Kodak High Contrast Copy Film (panchromatic)	over 225 lines/mm	Tungsten ASA 64

Concerning spectral sensitivity, published spectrograms for the above films show that all would work about equally well for recording the P-5, P-7, and P-11 phosphors.

A comparison between film resolution and lens resolution (Tables 5 and 2) shows the film as the limiting factor in resolution for a 16 mm time lapse data recording system. Kodak Plus-X Pan film will record a maximum of 135 lines per mm. Comparison of these figures with Table 4 showing maximum resolution which the Range Height Indicator scope of the Radar Set AN/CPS-9 requires, shows that the above system with Kodak Plus-X Pan film will

resolve everything the radar system will resolve on long pulse at any range, on short pulse up to 25 miles range, and up to 86.0% and 57.4% of the small bits of intelligence which the scope displays on short pulse at 50 and 75 miles range respectively. This film and lens system can resolve on the scope a dot no smaller than 0.162 mm in diameter.

This 0.162 mm diameter dot on the Range Height Indicator scope of the weather Radar Set AN/CPS-9 corresponds to a radial distance in the atmosphere of 17.4 meters on the ten mile range setting, 43.5 meters on the 25 mile range setting, 87.1 meters on the 50 mile range setting, and 130.6 meters on the 64 mile range setting. One half the transmitted pulse length limits the radial atmospheric resolution of the system to 75 meters on short pulse and to 750 meters on long pulse regardless of the range setting used on the scope. The researcher often uses some systematic method of gain reduction with weather radar for drawing isoecho contours (1, 29) and for finding the cores of precipitation cells (1). The above resolution figures set the limits of usefulness for gain reduction with the weather Radar Set AN/CPS-9 when determining echo size, separation, and intensity gradient. The Radar Set AN/CPS-9 Range Height Indicator photographic data recording system gives satisfactory results in the majority of cases where mode of operation of the radar uses long pulse on any range, or short pulse on ranges of less than 50 miles.

THE CATHODE RAY TUBE

After establishing a satisfactory camera, lens, film, and scope relationship, most satisfactory weather radar data collection requires some method for replicating the scope intensity such that a given incoming radar signal produces a given scope signal intensity which in turn appears as a corresponding given amount of density recorded on the film. A study of scope intensity as an indicator of echo strength, using a densitometer on the films or by drawing isoecho contours with a stepped gain control (29) requires a rigorously controlled intensity setting.

The following discussion of the cathode ray tube as a data display system helps in understanding the requirements of this type of system for rigorous intensity control.

A special type of vacuum tube forms the cathode ray tube (28). In it, electric or magnetic fields cause the cathode-emitted electrons to accelerate to high velocity, focus into a narrow beam, and direct themselves in an intelligent pattern to a chemically prepared screen which fluoresces at the point where the electron beam impinges (28, 33). Either electrostatic deflection plates or electromagnetic deflection coils control the pattern which the electron stream draws on the tube face (28). Since the electron beam has little mass, it takes little energy to deflect it (28).

A substance which has a low work function coats the cathode, hence it gives off electrons easily (28). A heater inside the cylindrical cathode indirectly raises the temperature of the cathode to the

point where electrons continually boil off the cathode surface. This builds up a cloud of free electrons just off the surface of the cathode. Anodes near the scope face set up a magnetic field which draws the electrons away from the cathode and toward the scope face (28, 33).

The first grid (Figure 1) controls the flow of electrons from the cathode. This grid consists of a cylinder which covers the cathode except for a hole in the end of the cylinder between the cathode and the scope face. A charge, negative with respect to the cathode, controls the number of electrons passing through the grid to the scope face. At the same time, the electrostatic field between the grid and the cathode helps to form the stream of electrons into a beam. Since the concentration of electrons in the beam striking the phosphor controls the intensity of the image on the scope face, and since the bias (negative charge) on the first grid controls the concentration of electrons in the beam, it follows that the bias on the first grid controls the intensity of the visual image which the phosphor produces. Indeed, this first grid bias usually performs the function of manual scope intensity control (28, 33). However, other factors, discussed later, also affect the scope intensity.

After leaving the first grid, the beam of electrons passes through the first and second anodes. The first anode, or focusing anode, focuses the stream of electrons into an even tighter beam than that which passes through the grid. The first anode has a positive charge with respect to the grid and cathode, but has a lower potential than the second anode. Therefore, it appears negative with respect to the second anode. The second anode, or accelerating anode, has

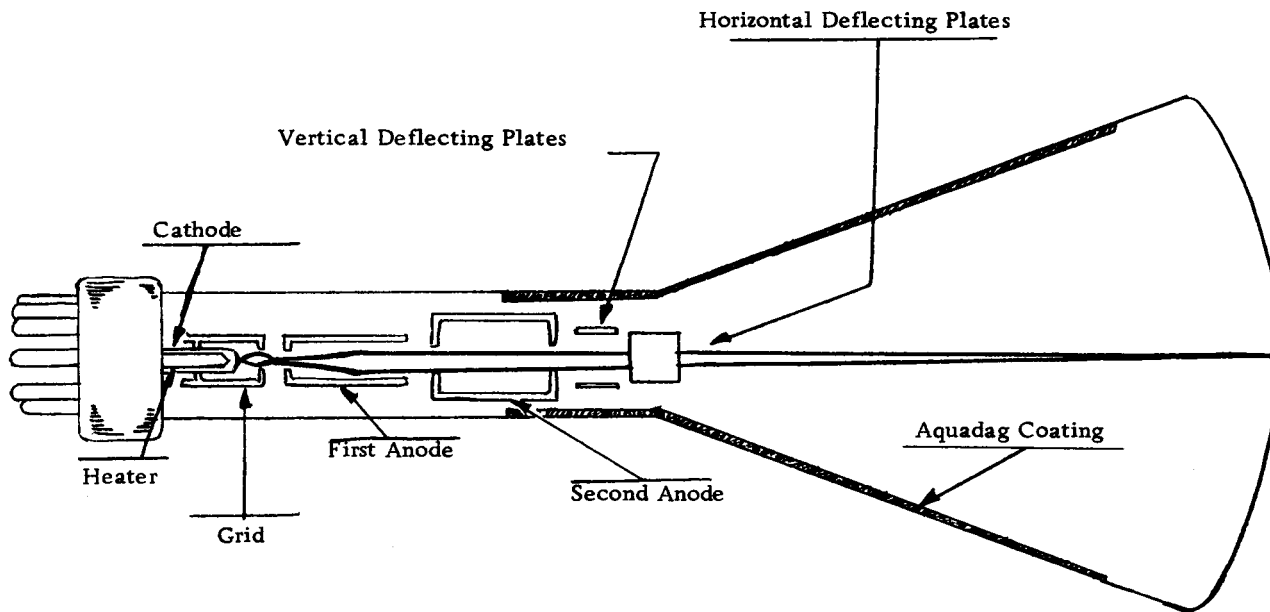


FIGURE 1. Typical Electrostatic Cathode Ray Tube Diagram.

a very positive bias with respect to the cathode, thus causing the electrons in the beam to accelerate rapidly on their path from the cathode to the field of the second anode. This field also helps focus the electron beam into a spot on the scope face (28, 33). A potentiometer varies the bias on the first anode, hence this anode acts as the primary focus adjustment (34).

Depending upon the design of the scope, the electrons then pass through a set of horizontal and vertical deflection plates, or through a deflection coil or yoke. This controls the path of the electron beam. With the electrostatic deflection plate, the charge on the deflection plates produces a controlled electrostatic field which bends the beam by an amount proportional to the charge (voltage) on the plates (28). The beam first passes through the vertical deflection plates which orient it to the correct vertical level on the scope face. The beam then passes through a set of horizontal deflection plates which place it in the correct horizontal position. Hence this allows accurate positioning of the beam to any point on the scope face (33).

With electromagnetic deflection, a current flowing through a deflection coil (yoke) sets up an electromagnetic field. This field then deflects the electron beam in the same manner as does the electrostatic field of the deflection plates. Since both deflection plates and coils control only the direction of the electron beam, they have no significant effect on the intensity of the resulting image (28).

An aquadag coating on the inside surface of the cathode ray tube envelope between the second anode and the scope face constitutes the third anode or intensifying anode (33). This anode has a very positive charge with respect to the cathode, grid, and the other anodes. The potential gradient between the cathode and the second anode accelerates the electrons initially. They focus into a fine beam directed in an intelligent pattern toward the scope face (phosphor). The potential gradient between the second anode and the intensifying anode then further accelerates the beam. The amount of light which a phosphor releases depends partially on the energy (velocity) of the electrons striking the phosphor. Hence the velocity of the electron beam, largely controlled by the bias on the second and third anodes and to a lesser extent by the first anode, partly controls the intensity of the final image (28). Indeed, in some cases, controlling the second and third anode biases rather than the grid bias controls scope intensity. However, the very high voltages on the third anode make it difficult to control, while the relatively low voltages on the grid make it more feasible to control intensity by controlling the grid.

In summary: the bias of the grid and of the second and third anodes controls the image intensity.

Useful photographic data recording systems require either rigid control or accurate measurement of the scope image intensity. Accurate intensity measurement allows intensity control with either the grid bias control or with a control on the bias of the second and third anodes.

The Planned Position Indicator and Range Height Indicator scopes in the Radar Set AN/CPS-9 have +680 volts on the accelerating anode (second anode), and +4700 volts on the final acceleration anode (34). These unregulated voltages allow a fluctuation in the input voltage to the radar to result in a fluctuation in the bias of the cathode ray tube anodes (34). Where the radar power comes from a good constant source of commercial power, few problems arise. However, where the radar set receives its power from field generators, often the case in research operations, these problems multiply. For example, a change of one volt at the 115 volt input results in a proportional change of 4.5 volts on the accelerating anode and of 31.4 volts on the final accelerating anode, resulting in a 35.9 electron-volt change in the energy of the electrons striking the phosphor.

The other voltages which control scope intensity come from regulated power supplies in the Radar Set AN/CPS-9 (34). After the operator sets them they remain constant.

Thus, in order to repeat a given scope intensity setting, the system must have meters attached to the voltages on the grid, the first accelerating anode, and the final accelerating anode. A table correlating the various voltages with the various intensities which they produce would provide the correct intensity setting. Assuming the components in the two circuits do not fail or change, a meter on either anode and a meter on the grid would probably suffice, since the changes in the anode voltages usually go in the same direction with a constant ratio between them. This requires at least

two meters per scope, wired in such a way that they do not affect the impedance balance of the circuit.

Further consideration shows that as a cathode ray tube ages, it tends to lose its brilliance (light output to signal energy input level ratio) because ions bombard the phosphor, and because the emission coating of the cathode deteriorates physically.

Both the phosphor and the electron emission properties of the cathode tend to change with the age of the tube even if the radar power supply provides constant bias voltages to the various elements in the tube which control the output of light of the scope. Hence the light output of a given tube decreases with age (28).

The low work function cathode coating produces more free electrons per power input than a non-coated cathode, thereby raising the efficiency of the cathode. All heated cathodes emit their electrons by the thermionic emission process. In this process, the hotter the cathode, the more electrons it releases. However, many possible cathode materials melt before they become hot enough to overcome their work functions at desired bias voltages. Sometimes, the combination of two metals (as tungsten with a thorium coating) will produce a cathode with an even lower work function than that of either metal alone. Hence thoriated tungsten provides a useful cathode material (28).

When in use, the constant heat of the coated cathode tends to boil off atoms as well as electrons. Therefore, the already thin coating of low work function metal tends to disappear with use. As this happens, the efficiency of the cathode decreases, resulting

in fewer electrons for a given grid-cathode bias. As the cathode boils away, it ejects fewer electrons into the electron beam for a given grid bias setting and anode voltage setting, hence the resulting image on the phosphor dims (28).

The atoms that boil off the cathode carry a charge. The mass of one of these ions exceeds that of an electron by several orders of magnitude. The anodes accelerate the ions in the same manner as the electrons, therefore the heavier ions strike the phosphor with much more kinetic energy and momentum than do the electrons. When this happens, an ion may simply strike the phosphor and stick to it, thereby masking a portion of the phosphor from further light emission when an electron strikes the ion instead of the phosphor beneath it. After many ions have struck and stuck, the phosphor becomes coated with a thin layer of ions, causing its emission efficiency to decrease rapidly (28).

In another effect of ion bombardment of the phosphor, the ion strikes so hard that it not only deposits itself on the scope face, but also knocks loose a portion of the phosphor material. This bombardment can remove both the phosphor coating from the tube face and also form a layer of ions which masks either the light output of the phosphor, or the electron input to the phosphor, or both (22). The term "ageing" denotes this time dependent deterioration of the component.

Electron bombardment of the phosphor also tends to knock some of the phosphor loose, but compared to ion bombardment, this causes almost negligible ageing.

Most cathode ray tubes contain ion traps to prevent ion bombardment of the phosphor. These ion traps never obtain 100% efficiency, however, and ion bombardment remains the principal cause of phosphor ageing (28). The more recent cathode ray tubes have an aluminized coating deposited on the inner surface of the phosphor, a material semitransparent to electron flow but opaque to ion flow. This coating protects the phosphor from ions which knock off phosphor particles from the scope face (28). But some ions still stick to the aluminized coating, making it opaque to electron flow. Thus, this method alleviates only part of the problems of ion bombardment phosphor ageing.

Measuring cathode ray tube intensity by attaching voltmeters to the bias settings of the anodes and grid, with a correlated set of intensity tables seems unsatisfactory since these tables contain a time dependent error factor: phosphor and cathode ageing. Also, the replacement of a given cathode ray tube requires the experimental derivation by film tests of the tables. Direct external measurement of the light output of the scope circumvents the ageing problem. Therefore, measuring the light output of the scope directly with some light measuring device seems a better way to maintain a consistent scope intensity setting. The "CRT (Cathode Ray Tube) Photometer" provides a simple, efficient means whereby the weather radar researcher may achieve constant film densities when he records a given returned radar signal strength photographically.

The following discussion covers the three types of photoelectric devices used to measure light and demonstrates that the photoconductor best suits the radar meteorologist's purposes.

PHOTOCELLS

Three types of photocells exist, each based on a different photo-physical effect:

- 1) The photoemission cell, a vacuum or low pressure gas-filled phototube;
- 2) The photovoltaic cell, as found in most photographic light meters;
- 3) The photoconduction cell, found in the newer battery powered photographic light meters.

All these cells have in common the photoelectric effect.

Theoretically, all metals exhibit the photoelectric effect if radiant energy of suitable wavelength impinges upon a clean surface of the metal (13). An internal photoelectric effect occurs in photoconductors and photovoltaic cells; an external one occurs in vacuum phototubes or phototubes filled with a rare gas.

According to the surface characteristics of the photosensitive material with which incident photons collide, the surface reflects, transmits and absorbs a certain number of photons on impact (30).

By Einstein's Law,

$$(12) \quad h\nu = \frac{1}{2} MV^2 + \phi e \quad \begin{matrix} (13) \\ (28) \\ (30) \end{matrix}$$

Where:

$h\nu$ = energy of photon of incident radiation moving through space with the velocity of light

$\frac{1}{2}MV^2$ = kinetic energy of the electron emitted from the surface by impact of the photon

ϕ_e = energy required to release the electron from the surface

ϕ = work function characteristic of a given material

ν = frequency of radiation

Einstein's Law shows the kinetic energy of the ejected electron independent of the intensity and directly proportional to the frequency of the incident radiation.

A given number of photons per unit area per second (intensity of incident light) striking a photocathode releases a proportional number of electrons from the irradiated metal (15).

In monochromatic light, all the photons have the same amount of energy (9, 27):

$$\text{Energy} = h\nu$$

Where: h = Planck's constant = 6.62×10^{-27} erg-second

Increasing the intensity of the light source increases the number of photons and hence the number of electrons ejected from the cathode surface and hence the amount of photocurrent. But the individual energy of the photons does not increase when the light intensity increases and therefore, the kinetic energy (velocity) of the ejected electron does not increase. Therefore, in order to produce any photocurrent, the incoming photons must have enough energy to overcome the work function required to release an electron. Any surplus energy above the work function transforms to kinetic energy of the ejected electron. The amount of energy required to release

the electron may exceed the energy which the photon carries if the electron resides initially in an energy state below the top of the electron distribution in the partly filled energy band of the cathode metal. Therefore, a given photocathode has a long wavelength threshold frequency. Hence, impinging light photons of frequencies lower than this threshold carry too little energy to release an electron, no matter how intense the incident light (30, 31).

Vacuum phototube

In the process of photoemission, a photosensitive cathode ejects electrons into the surrounding space. Vacuum phototubes operate on this principle. The incident light flux ejects a proportional number of electrons. A nearby positively charged anode collects them, and they cause a current flow in the circuit external to the device. A meter measures this current, giving an indication of the light intensity striking the photocathode (19).

In a simple triode amplifier, an incoming signal on the grid controls the flow (flux) of electrons which boil off the heated cathode (thermal emission), in such a manner that the electrons flow toward a positively charged plate with the grid acting as a variable gate which opens and closes in proportion to the strength of the incoming signal. A very low work function cold cathode easily releases electrons from the surface of a phototube. The control signal comes in, not to a grid in the form of an electrical pulse of energy carried on a wire, but instead in the form of an electromagnetic light wave or bundle of energy (photon). This photon strikes the cathode and in

stopping, gives up its energy in releasing an electron from the cathode surface. This electron accelerates to the plate, which collects it. Current then flows through the external circuitry. In this process, one photon releases one electron (15).

Low work-function metals such as cesium or cadmium compose almost exclusively the photoemission cathode materials. This allows photoemission from the longer light wavelengths as well as those in the blue and ultraviolet region.

The phototube, by nature of its operation, requires a high voltage, very low current power supply for the plate cathode bias (19). The bulky phototube and any system using it to measure the light intensity of a very small region of a constant signal reference point on the cathode ray tube, requires an associated lens system to focus that point on the photocathode. These factors outweigh the favorable characteristic of greater temperature stability than in either the photoconductor or the photovoltaic cell. The bulky vacuum phototube thus makes it impractical to use with the radar cathode ray tube for measuring the scope intensity.

Photovoltaic cells

The following discussion on photoconductors assumes the use of an intrinsic type semiconductor where the hole flow equals the electron flow (28). If instead, the cells has an n-type semiconductor, electron flow predominates in the charge flow. Or if the cell has a p-type semiconductor, hole flow predominates in the charge flow (18, 19, 30).

In the photovoltaic effect, light falling upon a rectifying contact or junction generates a voltage. This sensitive element may connect directly to an external load such as a meter with no power supply other than the incident light striking the photovoltaic cell (19).

The photovoltaic cell, e.g. lightmeter, comprises a small self-contained unit for the measurement of light intensities. However, the smallest of the photovoltaic cells has a sensitive area about 1/2 inch in diameter. For weather radar data collection, the lightmeter must measure some standard reference radar signal displayed on the scope. The desired method of producing this signal uses a radar signal generator test set. This signal produces a very small display on the scope. On the Radar Set AN/CPS-9, the resulting scope signal measures about one millimeter in diameter. Hence, most of the sensitive area of the smallest photovoltaic cells remains unilluminated by the standard reference signal, and the photographed light intensities fall below the useful range of the photovoltaic cells. The preliminary experiments performed with the Radar Set AN/CPS-9 using three different commercial photographic photovoltaic lightmeters, representing the more sensitive lightmeters of this type on the market, supported this conclusion.

Photoconductor cells

Photoconductivity cells operate by the process of photoconduction. In this process, light of a given wavelength falling on the surface of a semiconductor expends the energy carried by its photons to transfer electrons from the valence band of the semiconductor to

its conduction band (30). These transferred electrons then become conduction particles as do the free holes left behind in the valence band. Placing a bias voltage across the cell causes this light-induced increase in conductance to result in an increase in the current flow through the cell. The liberated charges increase the conductivity of the semiconductor element in the same ratio as the ratio of their number to the numbers of such particles present before the light became incident on the element (30). A constant intensity of light upon the cell continually liberates new electrons and holes (30).

The energy required to emit an electron from a photocathode surface exceeds that required to move an electron from the valence band to the conduction band (30). Hence a photoconductor of a given substance exceeds a photocathode of the same substance in sensitivity to the longer wavelengths of light (28).

In the photoconduction process, an electron-hole pair residing in the valence band of a semiconductor absorbs the impinging photon. If this photon comes from light above the threshold frequency, the electron then crosses the forbidden energy gap to the conduction band and the hole moves into the lower band with equal and opposite momentum. If, however, the work function of the material exceeds the quanta of energy of the photon, the semiconductor either acts transparent to the photon, reflects it, absorbs it and reradiates the energy as heat, or gives up the extra kinetic energy to a third body called a recombination center (30). A recombination center consists of a disturbance in the lattice structure of the crystal such as an impurity atom or ion which can either furnish or absorb the

momentum necessary to fulfill the conservation of momentum requirement for the recombination process (30).

If the photoelectric activation process, measurement of the energy of a free hole refers downward from the top of the lower band whereas measurement of the energy of a free electron refers upward from the bottom of the upper band. The forbidden gap lies between the lower and upper band, and in theory, a free electron or hole cannot reside in this gap (28, 30). After being freed by an impinging photon, the electron and hole separate with equal and opposite momenta, and hence equal energies. Thus the two particles should come to rest at equal energy levels. If the two particles do not come to rest at equal energy levels, a "forbidden transition" occurs. Assume an electron-hole pair lies originally at rest in a place where they can separate only by a forbidden transition, after absorbing a photon, the pair will separate momentarily then recombine. The photon releases its excess energy as another photon, as heat, or as momentum given to a recombination center (30).

If an electron starts to cross the forbidden band but has insufficient energy it normally returns to the valence band. However if another thermally excited electron strikes the electron from the correct direction, the freed electron continues through the forbidden gap to the conduction band, thus increasing the conductivity of the material. The chances that this will happen greatly increase as the temperature of the semiconductor increases, because of the increased thermal excitation of the electrons residing in the semiconductor. Hence, in a semiconductor, an increase in temperature

can result in an increase in conductivity (28, 30).

If the semiconductor performs the function of a photoconductor in a light meter without temperature compensation or correction, distinguishing whether a change in current occurs from a change in light intensity, a change in temperature, or from both, presents great difficulty.

In summary, external measurement of scope intensity requires a photosensor. Three types exist: 1) the vacuum phototube, 2) the photovoltaic cell, and 3) the photoconductor cell.

The vacuum phototube has the most temperature stability, however, its physical size requires an optical system in conjunction with the tube for measuring the small points of light from the scope. It also requires a separate plate power supply.

The photovoltaic cell requires no external power supply. Its temperature instability characteristics closely resemble those of the photoconductor. It has less sensitivity than either the vacuum phototube or the photoconductor. The maximum area metered on the scope measures about 1 mm by 1 to 10 mm, while the sensitive area of the smallest photovoltaic cell approximates 1/2 inch in diameter. Hence, the image covers only a fraction of the sensitive area of the cell. This makes the photocell too insensitive to use in measuring a calibrated intensity area of the scope.

The photoconductor comes available with sensitive areas about 1 mm by 4 mm. It requires a very low current bias voltage. Batteries perform well as the bias supply.

CRT PHOTOMETER

Taking these facts into consideration, the author designed the CRT Photometer for use with the Radar Set AN/CPS-9 at McCulloch Peak, using a Clairex Cl-2p photoconductive cell. The circuit diagram (Appendix II, Figure 5) shows that the circuit does not compensate for temperature, and that the same meter which reads the light level in micro-amperes of photocurrent also can read the external bias control adjustment.

Appendix V shows published temperature characteristic information on the CL-2p and other photoconductive cells. Figure 27 shows the results of a temperature versus photometer reading at a mid-scale light level reading performed from 34^oF to 122^oF. This curve shows that temperature changes within the normal operating range of the CRT Photometer produce no significant effect on the scope intensity reading.

With the external bias (calibrate) control, the bias voltage can operate at different levels as necessary in order to use the CRT Photometer with other scopes or even other radar units. Biasing the cell well below the battery voltage allows the bias control to compensate for changes in the battery voltage with age or temperature. Use of a Zener diode in the power supply would automatically maintain a constant bias voltage (Appendix II, Figure 7).

Three examples of photographs taken with the aid of the CRT Photometer appear in Appendix I.

Figure 2. Range Height Indicator scope on the Radar Set AN/CPS-9.

Figure 3. Plan Position Indicator on the Radar Set AN/CPS-9.

Figure 4. Range Height Indicator presentation from an SO-12N radar located in the Cascade Mountains during the summer of 1963.

In all cases, a prominent area of ground clutter represents the standard signal photographed. Although this use of a ground clutter object as a standard gives reasonably good photographic results, seasonal changes in foliage, snow cover, or moistness of the object may cause changes in the percent reflection from that object. A signal of known strength from a signal generator to the radar system from some outside point would give more constant results. This would allow quantitative analysis of the film density to returned signal strength relationship. The CRT Photometer determines the scope intensity, which can act as a constant, as it reads the test signal.

Regardless of the type of standard signal chosen, after acquiring a CRT Photometer a series of film tests allow determination of a meter reading which will act as the intensity standard for the scope. Thus, the weather researcher may obtain consistent, accurate photographic records of the radar scope display.

SUMMARY EXAMPLE

In setting up and using a photographic data recording system for weather radar, the researcher should take the following steps:

1. Determine the normal mode of operation of the radar, then calculate the required scope resolution using either of the formulas

$$13) \quad R^* = \frac{B r^* K}{L}$$

$$14) \quad \text{or} \quad R^* = \frac{r^* K'}{h L}$$

The second equation gives more accurate results since the first equation may give too large a value depending on the Intermediate Frequency amplifier design of the radar.

2. Compute the theoretical resolution of the lens at that f/stop setting for the distance where the image area covers the bezel and scope object area.

3. Compute the theoretical resolution of the lens at that f/stop, or if possible, obtain the information from the lens manufacturer.

4. Find the resolution at the required image size using the magnification formula:

$$15) \quad M = \frac{s'}{s} \quad , \quad \text{and} \quad 16) \quad R = OM$$

5. Compare this value with the lens resolution. If the lens resolution surpasses or equals the value (R) above, select a film which meets the resolution requirements.

6. Construct the system if it meets the theoretical requirements.

7. Construct a photoconductor cell-type light meter to measure the light intensity of the cathode ray tube at standard radar signal levels.

8. Calibrate the system by measuring the light intensity of the image of an area of fixed ground clutter or of a signal generator test signal. The test signal gives the most reliable comparison between radar return signal recorded as film density, and echo strength.

9. Adjust the scope intensity to the correct value for the photographic system, using the photometer measurements.

10. Collect data.

CONCLUSIONS

By applying the equations discussed in this paper, the researcher could design a photographic data collection system which would record all the information that the scope displays for the mode of operation of a given radar set.

Application of these equations to the Range Height Indicator photographic data recording system on the weather Radar Set AN/CPS-9 at McCulloch Peak, Oregon, shows that this system resolves everything the radar system will resolve on long pulse at any range, on short pulse up to 25 miles range, and 86% and 57% of the small bits of information which the scope displays on short pulse at 50 and 75 miles range respectively when using Kodak Plus-X Pan film. This film and lens system can resolve on the scope a dot having no smaller diameter than 0.162 mm. This corresponds to a radial distance in the atmosphere of 17.4, 43.5, 87.1 and 130.6 meters on the 10, 25, 50, and 75 mile range settings respectively. One half the transmitted pulse length limits the radial atmospheric resolution of the system to 75 meters on short pulse and to 750 meters on long pulse regardless of the range setting used on the scope. This system then gives satisfactory results in the majority of the cases where the mode of operation of the radar uses long pulse on any range, or short pulse on ranges of less than 50 miles.

A photoconductive cell type lightmeter, used with a standard strength radar signal provided by a prominent area of ground

clutter or a radar signal generator test set yields the information necessary to enable the radar operator to maintain a constant scope intensity-echo strength relationship. The photographic system records this as a constant scope intensity-film exposure density relationship.

SUGGESTIONS FOR FUTURE RESEARCH

The time lapse photography method of collecting weather radar scope presentations often leaves the researcher with more film data than he has time to reduce and analyze. In one current method of film analysis, the data reducer projects the film image upon a rectangular coordinate graph representing the slice of the atmosphere he wishes to study. He then tediously marks each square with a signal-no signal indicator for each frame. After many frames, the analysis proceeds with this reduced data.

The author suggests that a bank of photocells in conjunction with a bank of flip-flop circuits feeding a bank of digital counters could vastly decrease the time spent in the above type of data reduction. Possibly, a Vidicon tube used with a digital read-out system would perform better than a bank of photocells in activating the counters. Either of these systems mated with a computer card or tape puncher could save yet another manual step.

For a study requiring only the average signal for a long time span, the author suggests that the method of photointegration shows promise. This technique consists of projecting many time lapse frames onto one single transparency. A densitometric analysis of the transparency then gives the average signal strength per unit time relationship.

The author feels that any automated or semiautomated method of film data reduction, even though expensive at first, would pay for itself many times over in the progressive savings of man hours.

GLOSSARY

AGEING: Loss of component efficiency as the component deteriorates with age.

AQUADAG COATING: A conductive coating on the inner surface of a cathode ray tube envelope near the phosphor end which acts as a final electron accelerating anode.

BANDPASS, BANDWIDTH: Frequency range which an amplifier will accept; the width of the frequencies which fall within the three decibel rolloff on the frequency response curve.

BEZEL: Information surrounding the radar scope, necessary for interpretation of radar films, photographed with the scope, and replacing a written log.

CENTRAL LENS PLANE: A plane in the lens system from which the focal length, image, and object distances are measured. In a thin lens, this plane passes through the center of the lens. In a compound lens, the iris diaphragm approximates this plane.

CHROMATIC ABERRATION: A defect in a lens which causes light of different colors (wavelengths) to focus at different image planes.

DEPTH OF FIELD: The distance between objects nearest and farthest from the lens which remain in focus.

FORBIDDEN GAP: An energy band between the valence band and the conduction band in a material where an electron can not remain.

FORBIDDEN TRANSITION: A process which would cause an electron to reside in the forbidden gap.

HALATION: Light spreading from the bright portion of an image into the surrounding dark portion, caused by reflection from the surface supporting the film emulsion or scope phosphor.

IRIS DIAPHRAGM: A number of thin overlapping metal leaves in the lens adjustable to produce apertures of given f /stops.

LUMINANCE: The amount of light emitted or reflected from an area to be photographed; luminance range = brightness range = contrast.

PHOSPHOR: A coating on the inner surface of the scope face which emits light when an electron beam strikes it.

SCOPE PERSISTENCE: The length of time the image remains visible on the scope.

SPHERICAL ABERRATION: A defect in a lens which causes light passing through the periphery of a lens to focus in a different plane than that passing through the lens center.

WORK FUNCTION: Energy required to release an electron from a surface.

BIBLIOGRAPHY

1. Battan, Louis J. Radar meteorology. Chicago, University of Chicago Press, 1959. 161p.
2. Clairex Corporation. Clairex photoconductive cells. New York, 1963. 15p. (no. 100CL363A)
3. Cole, R.S. A treatise on photographic optics. London, Sampson Low, Marston, n.d. 330p.
4. Conrady, A. D., et al. Photography as a scientific implement. New York, D. Van Nostrand, 1923. 549p.
5. Decker, Fred W., et al. Investigation of instrumentation and techniques for army weather observation. Corvallis, 1962. 18p. (Oregon State University, Atmospheric Science Branch of Science Research Institute. Report no. 3, Third Quarterly Progress Report, 1 Aug. through 31 Oct. 1962. Signal Corps Contract no. DA-36-039 SC-89186. Continuation of contract DA-36-039 SC-78918. DA Project no. 3A99-27-005-07)
6. Fosberg, Michael Allen. A synoptic and radar study of post-cold-frontal squall lines. Master's thesis. Corvallis, Oregon State University, 1962. 107 numb. leaves
7. Eastman Kodak Company. Kodak films in rolls. Rochester, 1962. 28p. (Kodak Publication no. F-13)
8. _____ Kodak plates and films for science and industry. Rochester, 1962. 28p. (Kodak Publication no. P-9)
9. Hughes, Arthur Llewelyn, and Lee Alvin Dubridge. Photoelectric phenomena. New York, McGraw-Hill, 1932. 531p.
10. Hunter, Marvin N. Simple radar scope photography. Weatherwise 7:38-40. 1954.
11. International Telephone and Telegraph Corporation. Reference data for radio engineers. 4th ed. New York, American Book-Stratford Press, 1956. 1121p.
12. James, T.H. and George C. Higgins. Fundamentals of photographic theory. New York, Morgan and Morgan, 1960. 345p.
13. Kaplan, Irving. Nuclear physics. Reading, Mass., Addison-Wesley, 1955. 609p.

14. Lamb, Robert C. and John V. McFadden. United States Forest Service Fire-Weather Project. Corvallis, Oregon State University, Feb. 1, 1964. 8 numb. leaves (Progress Report to Atmospheric Science Branch of Science Research Institute) (Typewritten)
15. Lange, Bruno. Photoelements. New York, Reinhold, 1938. 297p. (Translated by Ancel St. John)
16. Ligda, Myron G.H. Radar scope photography. Cambridge, Mass., 1947. 63p. (Massachusetts Institute of Technology. Technical Report no. 4)
17. . Special radar scope cameras. Cambridge, Mass., Department of Meteorology, 1951. 41p. (Massachusetts Institute of Technology. Technical Report no. 11)
18. Mann, George B. ABC's of transistors. Indianapolis, Howard W. Sams & Company, Bobbs-Merrill, 1959. 96p.
19. Mark, David. Basics of phototubes and photocells. New York, John F. Rider, 1956. 128p.
20. Meagher, John R. and Art Liebscher. TV servicing. Harrison, N. J., Radio Corporation of America, 1951. 45p.
21. Mees, C.E. Kenneth. The theory of the photographic process. New York, Macmillan, 1942. 1124p.
22. Mendenhall, Laurence David. Variability of precipitation in western Oregon as revealed by radar echo patterns. Master's thesis. Corvallis, Oregon State University, 1961. 39 numb. leaves
23. Mortimer, F.J. Wall's dictionary of photography and reference book for amateur and professional photographers. 15th ed. London, Illiffe and Sons, n.d. 701p.
24. Pembroke, John D. RHI camera hood and bezel assembly for AN/CPS-9 weather radar set. Corvallis, 1962. 9 numb. leaves (Oregon State University. Atmospheric Science Branch of Science Research Institute. Undergraduate Research Participant report to National Science Foundation)(Typewritten)
25. Radio Corporation of America. RCA phosphors for cathode ray tubes, black-and-white and color picture tubes, and other applications. Harrison, N.J., 1961. 19p. (Form no. TPM-1508A)

26. _____, RCA photocells, solid-state photosensitive devices, data circuits characteristics. Harrison, N.J., 1963. 31p. (Booklet ICE-261A)
27. Rossi, Bruno. Optics. Reading, Mass., Addison-Wesley, 1957. 510p.
28. Ryder, John D. Electronic fundamentals and applications. Englewood Cliffs, N.J., Prentice-Hall, 1950. 814p.
29. Sarmah, Suryya Kanta. A radar and synoptic study of rain at a point. Master's thesis. Corvallis, Oregon State University, 1963. 72 numb. leaves
30. Shive, John N. The properties, physics, and design of semiconductor devices. Princeton, N.J., D. Van Nostrand, 1959. 487p. (Bell Laboratory Series)
31. Summer, W. Photosensistors. London, Chapman & Hall, 1957. 675p.
32. U.S. Air Force. Extension Course Institute. Ground electronics officer, course 3002. Vol. 2. The AN/TPS-10D. Gunter Air Force Base, Alabama, Feb. 1956. 237p.
33. U.S. Dept. of the Army. Oscilloscope I-245-A. Washington, D.C., 1959. 49p. (Technical Manual TM11-2689A)
34. U.S. Dept. of the Army and Dept. of the Air Force. Radar set AN/CPS-9, field maintenance. Washington, D.C., 1956. 494p. (Dept. of the Army Technical Manual TM11-1504. Dept. of the Air Force Technical Order TO31P6-2CPS9-2)
35. Waddell, John H. Depth of field tables. R/D-Research Development 15(4):59-60. 1964.

APPENDICES

APPENDIX I
BEZEL CONSIDERATIONS

APPENDIX I

BEZEL CONSIDERATIONS

The bezel displays the information necessary for later interpretation of the radar scope pictures. The same film frame records both the radar scope picture and the bezel, hence the same considerations in recording the scope apply to the bezel. The bezel has its own illumination difficulties.

Two basic methods for composing a bezel include: 1) Banks of lights having given coded meanings, or banks of light illuminating small photographic transparencies from behind, thus eliminating the need for a code; 2) Opaque dials, cards or clocks. In combination, these present information difficult to present with only the lighted banks (5, 24).

When using illuminated transparencies or light banks, the failure of a light may present misleading bezel information. More serious problems arise because of light failure in a code system than in the transparency system. Use of two lamps to illuminate each transparency eliminates this possible error source in the transparency system. The operator notices the intensity decrease produced when one of the bulbs burns out, and he replaces it. At the same time the film still records the half-lighted transparency. When using an information strip with one light always on, either the operator or the person analyzing the film sees that a lamp has failed, and adjusts his observations accordingly (24).

In the Range Height Indicator camera assembly of the Radar Set AN/CPS-9 at McCulloch Peak, Oregon, neon (NE-2) bulbs back-light negative photographic transparencies. These transparencies indicate the following information (5, 24):

A set of four neon lights automatically shows the range mark interval.

Nine lights automatically indicate the decrease in decibels of the receiver gain due to the step gain control.

Two bulbs illuminate the letters "STC" when using the sensitivity time control. Two bulbs illuminate "STC" as a safety factor since they probably will not both burn out at once. On the other indicators, the analyst notes a blank position on the film, easily determines from the other frames which bulb burned out, and then uses the blank position as a number.

Small neon bulbs prove useful for bezels because of their long life, small size, and low current drain. A current-limiting resistor in series with the bulbs controls to some degree the light output of the bulb. Plastic or film density filters placed between the transparency and the light provide further coarse attenuation of the light if necessary. Illumination of opaque dials, cards and clocks for bezel information must avoid surface reflection which makes portions of the dials unreadable due to glare (24). Also, white letters on black paper photograph better than black letters on white paper (17).

Preferably, both the bezel and the scope should lie in the same or nearly the same plane to reduce the problem of inadequate depth of field.

Shielding the scope face from the light which illuminates the bezel data cards prevents reflection from both the scope face and the scope phosphor. Place the shield around the scope face so that the data photograph shows only the edges of the shields (24).

A meter on the voltage supply for the data card lights allows adequate adjustment of the bezel light intensity to correspond with the scope intensity in use (24).

The following equations allow the necessary calculation of depth of field in designing a bezel:

$$17) \quad H = \frac{F^2}{fd} \quad (35)$$

$$18) \quad s_n = \frac{Hs}{H + (s - F)} \quad (35)$$

$$19) \quad s_f = \frac{Hs}{H - (s - F)} \quad (35)$$

Where:

H = the hyperfocal distance.

F = the focal length of the lens.

f = the f/stop number setting (aperture) of the lens.

d = the diameter of the circle of confusion at the film plane.

s = the distance focused upon; the distance from the effective central lens plane to the object plane focused on.

s_n = the distance to the near edge of the depth of field; the distance from the effective central lens plane to the nearest object resolved for a given circle of confusion \underline{d} .

s_f = the distance to the far edge of the depth of field;
 the distance from the effective central lens
 plane to the farthest object resolved for a given
 circle of confusion \underline{d} .

Applying these equations to the Range Height Indicator camera and bezel assembly of the Radar Set AN/CPS-9 at McCulloch Peak shows that when: $F = 20$ mm, $f = 8$, $s = 457.2$ mm, $d = 0.0037$ mm corresponds to the maximum resolution value for Kodak Plus-X Pan film; then $s_n = 443$ mm and $s_f = 473$ mm. This depth of field exceeds the requirements for the curvature of the scope face but not the bezel at this circle of confusion value.

Since the closest portion of the bezel measures 413 mm from the central lens plane, further application of these equations shows the circle of confusion in the film plane for this portion of the bezel as 0.0123 mm. This corresponds to a maximum resolution on this portion of the bezel of 2.07 lines per mm, which exceeds the requirements of this bezel.

Placing the bezel away from the scope face and then, with prisms or first-surface mirrors and a lens (if necessary), allows the image of the apparent bezel to fall in the same effective plane as the scope (17). This method eliminates both the depth of field problem and that of shielding the scope face from the bezel illumination. Using this method requires extreme care in servicing the bezel assembly. If a mirror gets misaligned, the bezel effectively shifts position. The author prefers to mount the bezel alongside the scope physically rather than optically if depth of field considerations will permit it. However, the design of some radar consoles

makes this impossible, and hence requires the use of mirrors.

The following pictures show examples of bezels and scope displays. In all three cases, the CRT Photometer provided the information for the scope intensity adjustment.

Figure 2, the Range Height Indicator (RHI) Scope and Bezel Assembly, Radar Set AN/CPS-9 located at McCulloch Peak, Oregon shows:

Scope display: precipitation and ground clutter echoes.

Stepped receiver gain setting (Stepped Gain Control): zero decibels (-DB) below maximum gain (full gain).

Range mark interval: five (5) statute miles.

Pulse length: short (S).

Antenna Azimuth: 134 degrees.

Time: 12:26 PM, PST (Pacific Standard Time).

Date: 30 March 1963.

Frame number: 37282.

Figure 3, the Plan Position Indicator (PPI) Scope and Bezel Assembly, Radar Set AN/CPS-9 located at McCulloch Peak, Oregon shows:

Scope display: precipitation and ground clutter echoes.

Stepped receiver gain setting: three (3) decibels below maximum receiver gain.

Range mark interval: five (5) statute miles.

Pulse length: short (S).

Antenna elevation: one degree.

Time: 11:27 AM, PST (Pacific Standard Time).

Date: 29 March 1963.

Frame number: 32457.

Figure 4, the Range Height Indicator (RHI) Scope and Bezel Assembly, SO-12N Radar Set located in the Oregon Cascade Mountains shows:

Scope display: chaff echoes and noise.

Antenna azimuth: five degrees.

Time: 1:42 PM, PST.

Range mark interval: one (1) nautical mile.

Frame number: 2265.

Date: 4 September 1963.

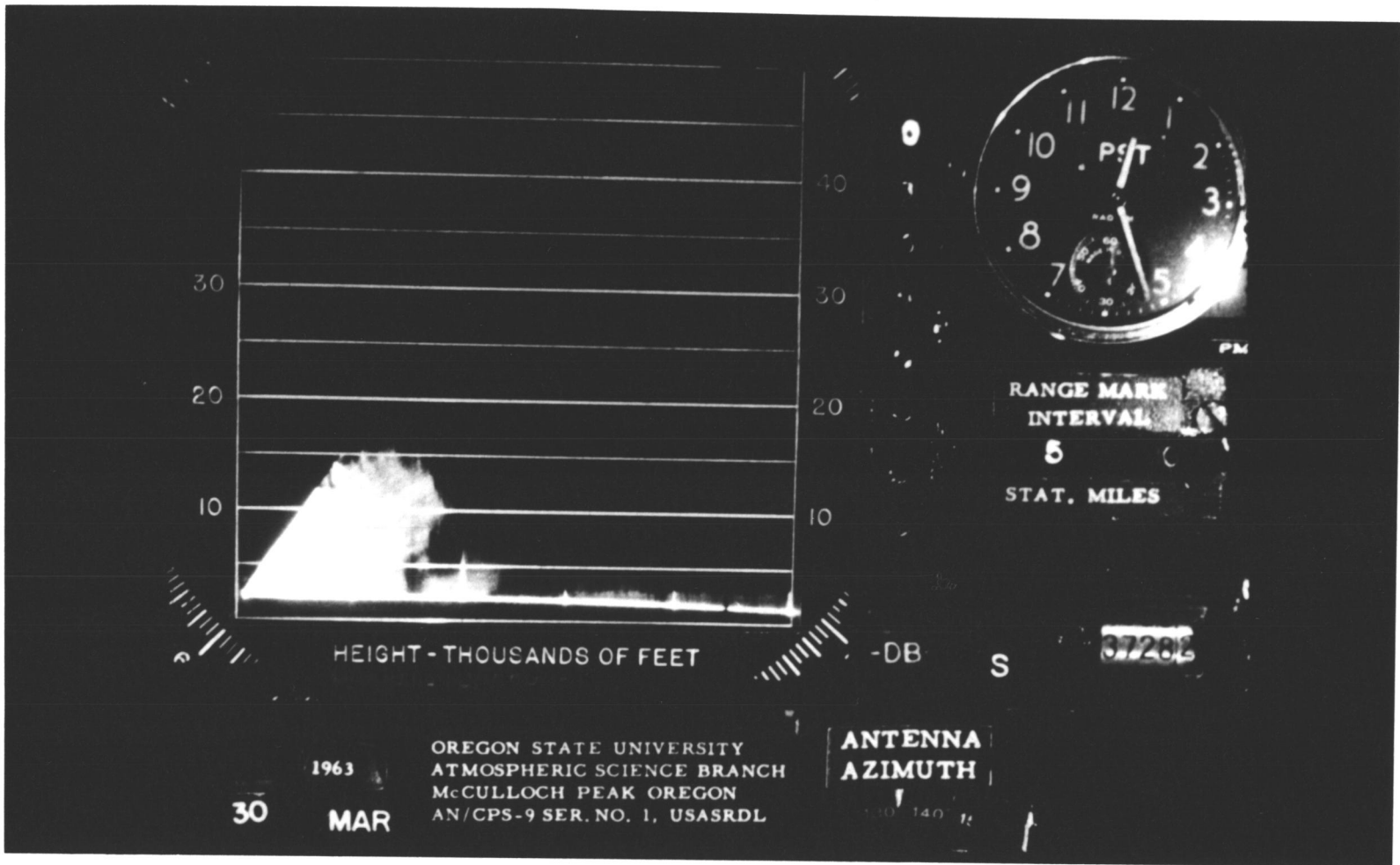


FIGURE 2. Range Height Indicator (RHI) Scope and Bezel Assembly, Radar Set AN/CPS-9.

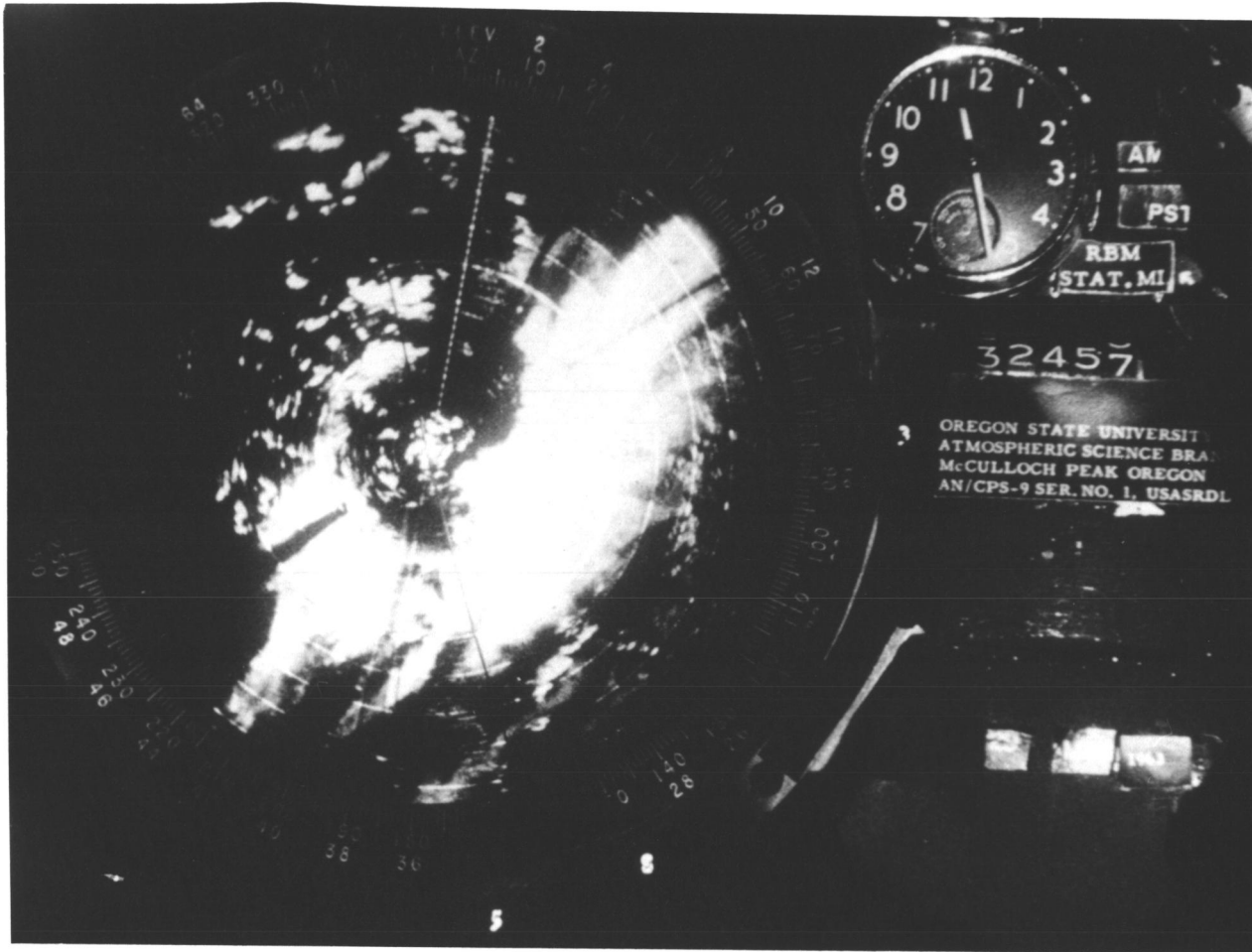


FIGURE 3. Plan Position Indicator (PPI) Scope and Bezel Assembly, Radar Set AN/CPS-9.

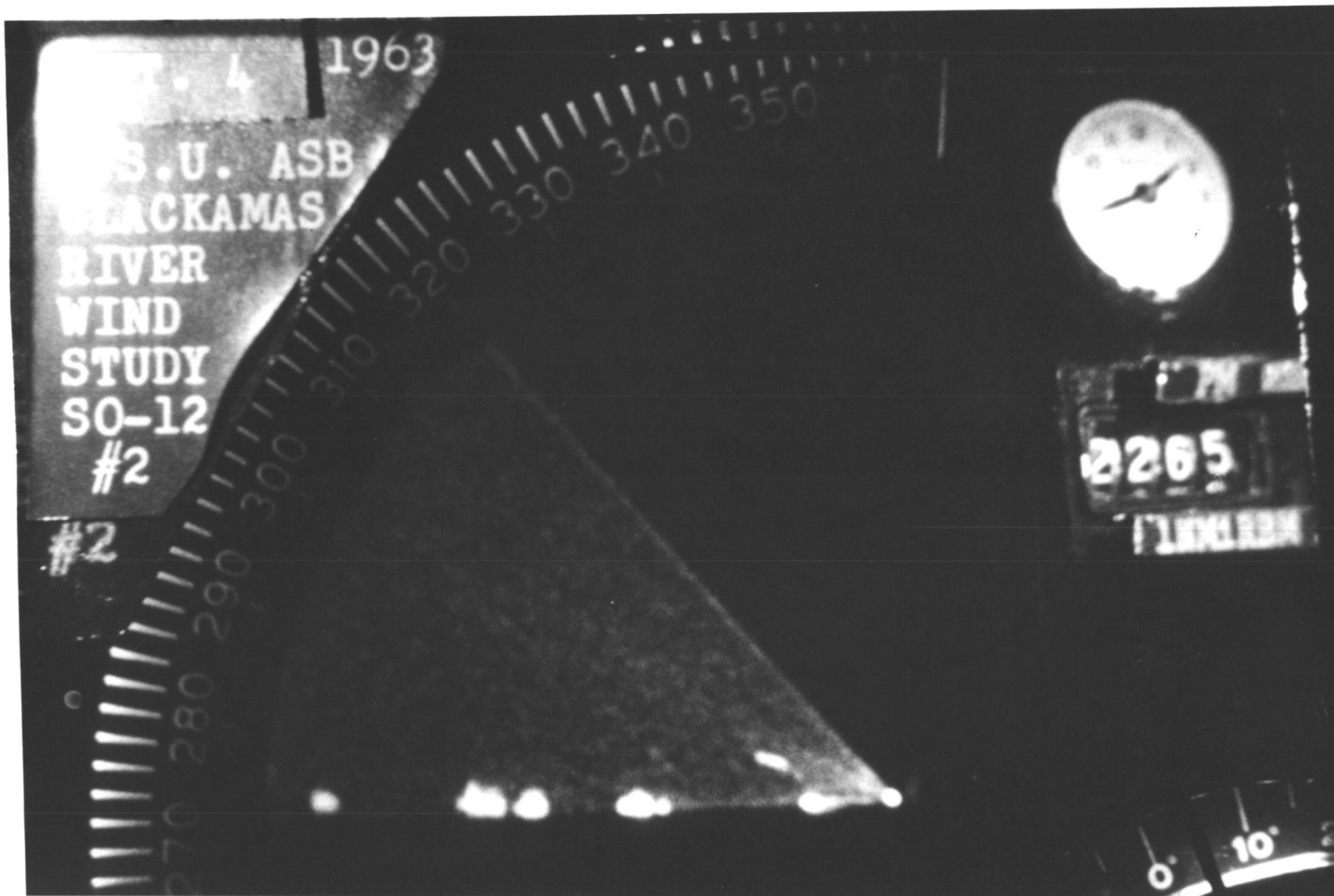


FIGURE 4. Range Height Indicator (RHI) Scope and Bezel Assembly, SO-12N Radar Set.

APPENDIX II
THE CRT PHOTOMETER



FIGURE 5. The CRT (Cathode Ray Tube) Photometer.

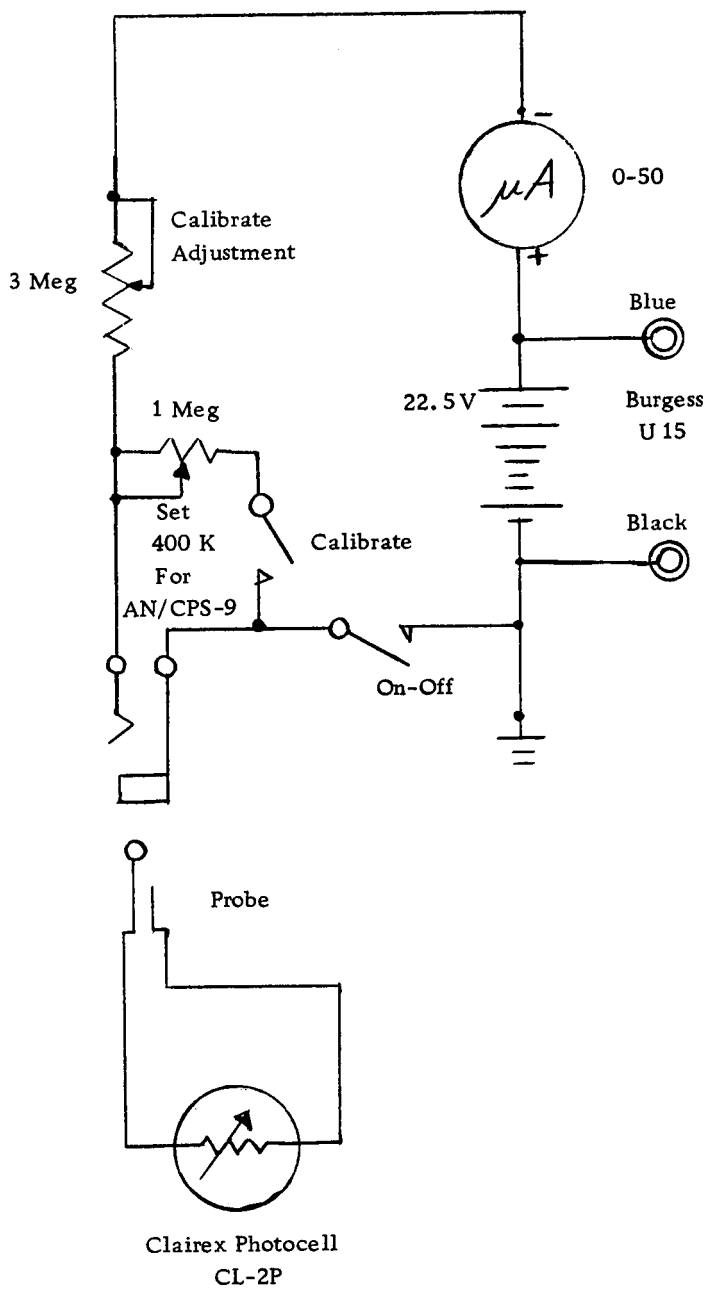


FIGURE 6. CRT Photometer Circuit Diagram.

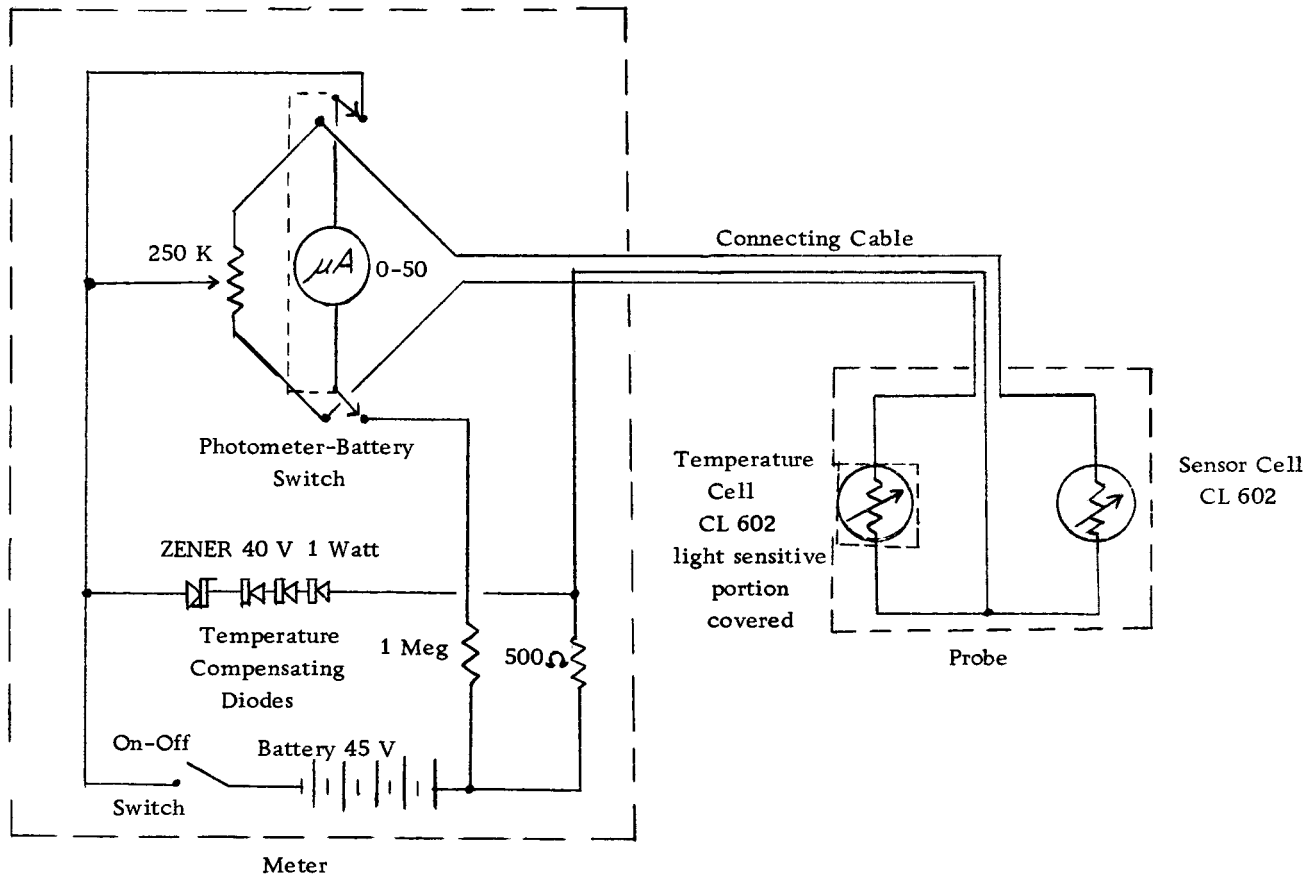


FIGURE 7. Proposed Improved CRT Photometer Circuit Diagram.

APPENDIX III
VISIBILITY CHARACTERISTIC OF THE HUMAN EYE

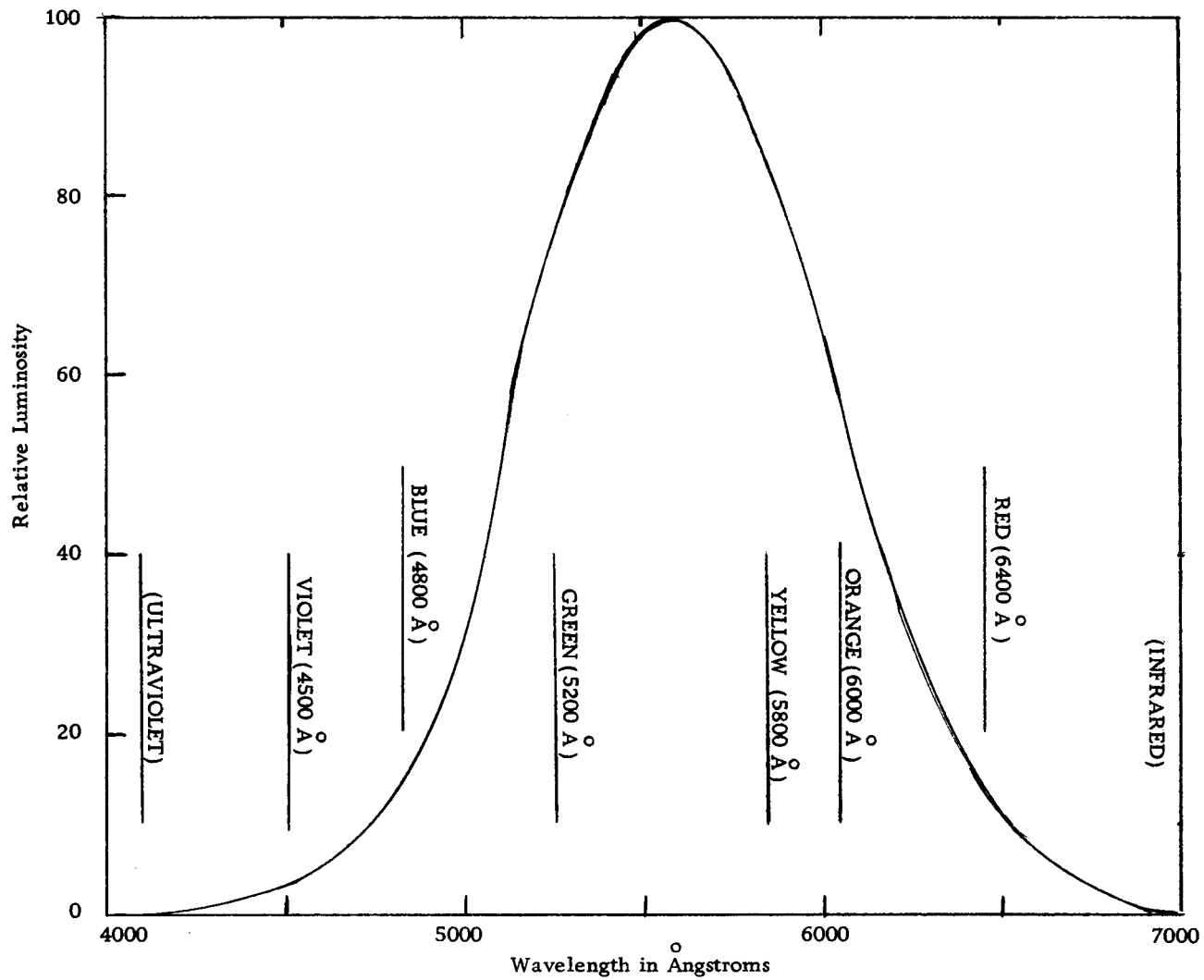


FIGURE 8. Visibility Characteristic of the Human Eye (26, 27).

APPENDIX IV
SPECTRAL ENERGY EMISSION CHARACTERISTICS
OF PHOSPHORS

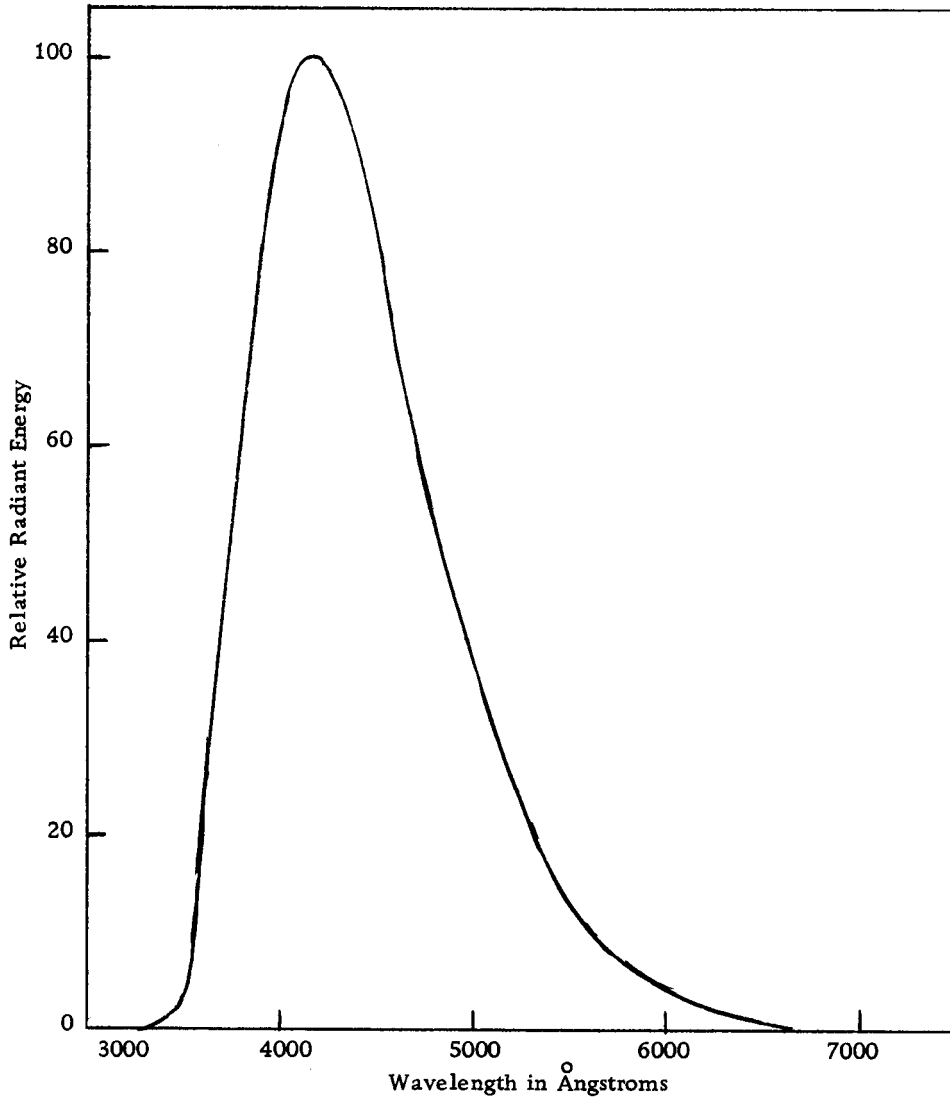


FIGURE 9. Spectral-energy Emission Characteristics of the RCA Phosphor P-5 (25).

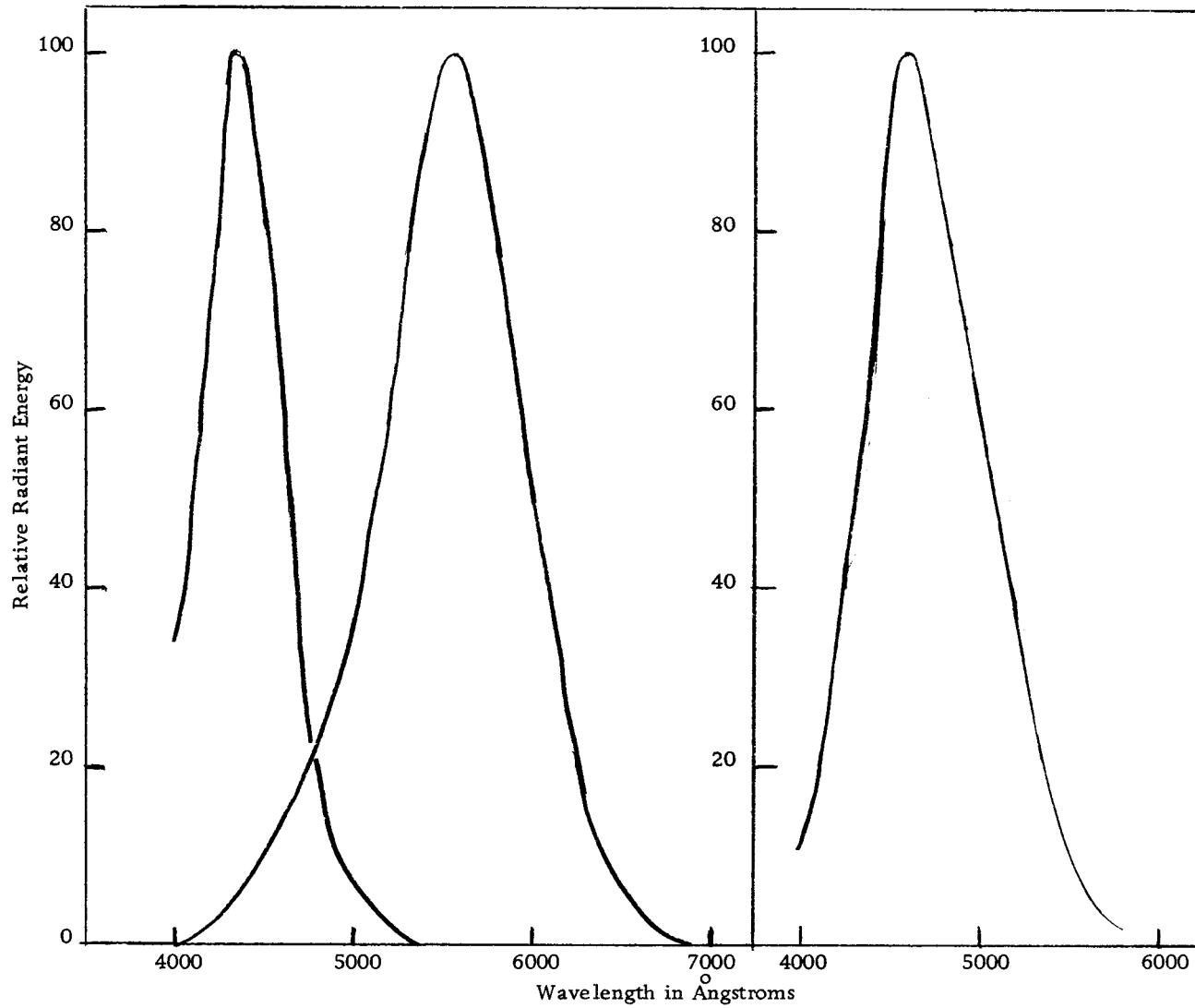


FIGURE 10. Spectral-energy Emission Characteristics of the RCA Phosphor P-7 (25).

FIGURE 11. Spectral-energy Emission Characteristics of the RCA Phosphor P-11 (25).

APPENDIX V
CHARACTERISTICS OF PHOTOCELLS

Spectral Absorption Characteristics of Photocells

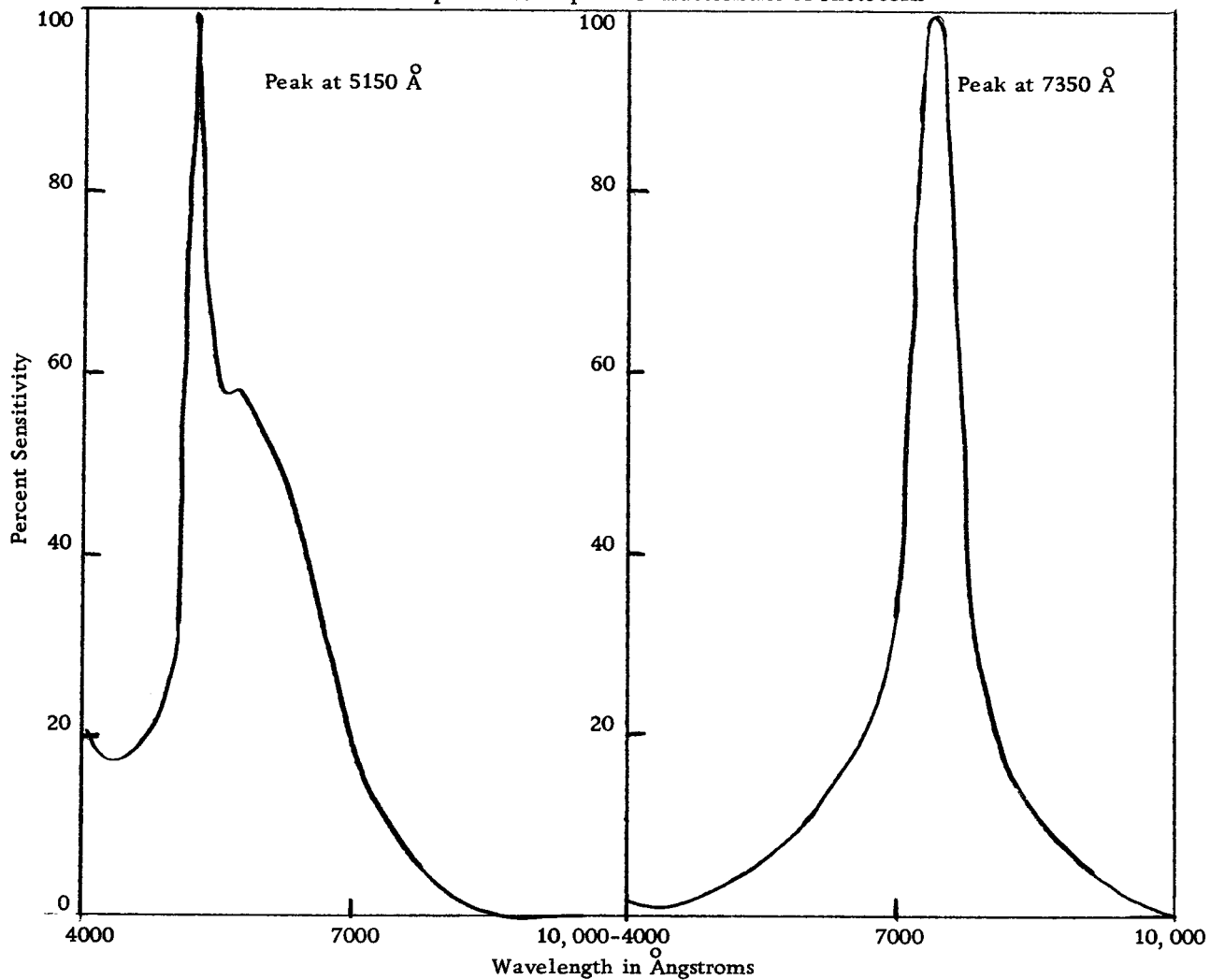


FIGURE 12. Clairex Type 2 Photoconductor Cell
Cadmium Sulfide (2).

FIGURE 13. Clairex Type 3 Photoconductor Cell
Cadmium Selenide (2).

Spectral Absorption Characteristics of Photocells

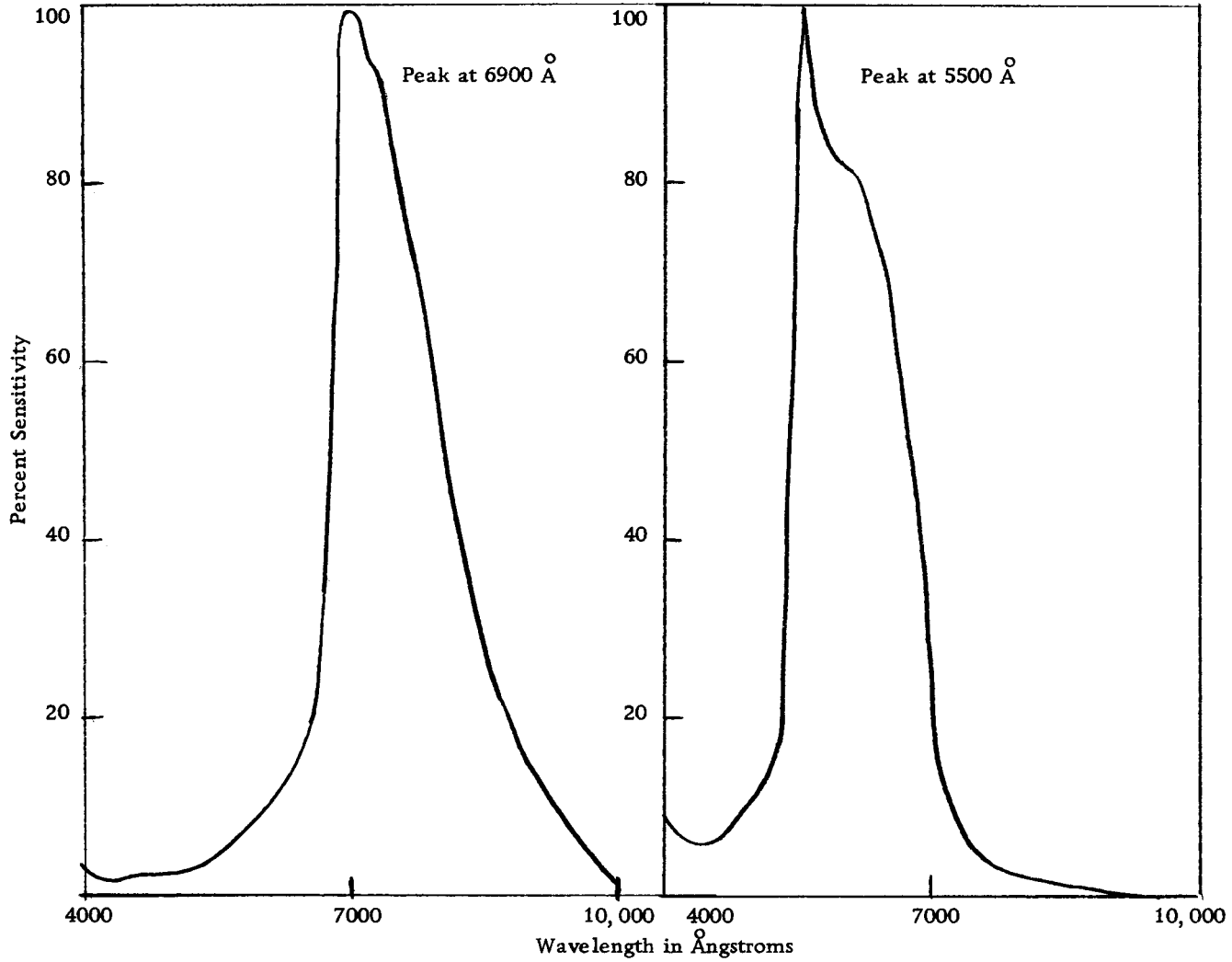


FIGURE 14. Clairex Type 4 Photoconductor Cell
Cadmium Selenide (2).

FIGURE 15. Clairex Type 5 Photoconductor Cell
Cadmium Sulfide (2).

Spectral Absorption Characteristics of Photocells

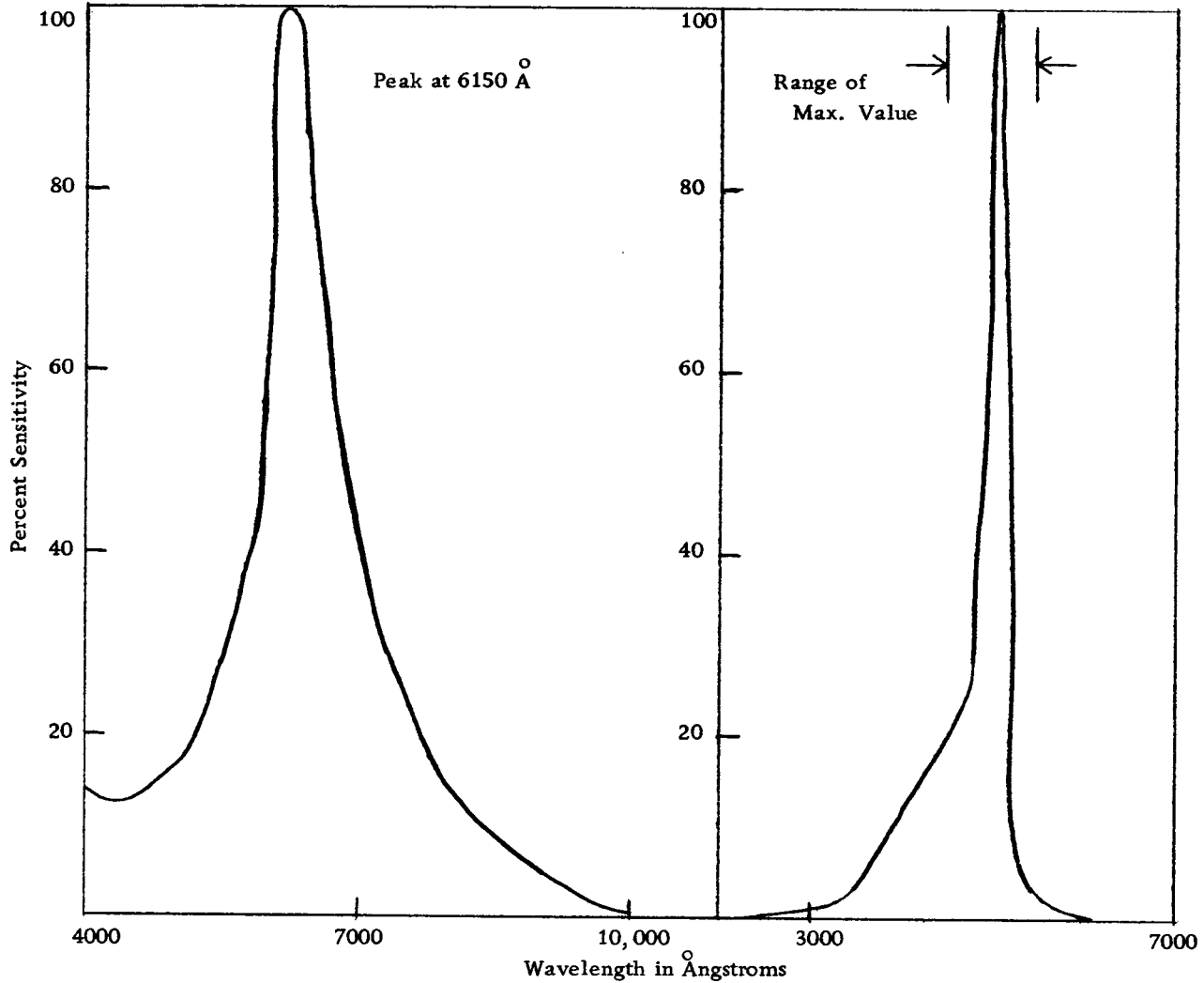


FIGURE 16. Clairex Type 7 Photoconductor Cell
Cadmium Sulfide (2).

FIGURE 17. RCA S-12 Photoconductor Cell (26).

Spectral Absorption Characteristics of Photocells

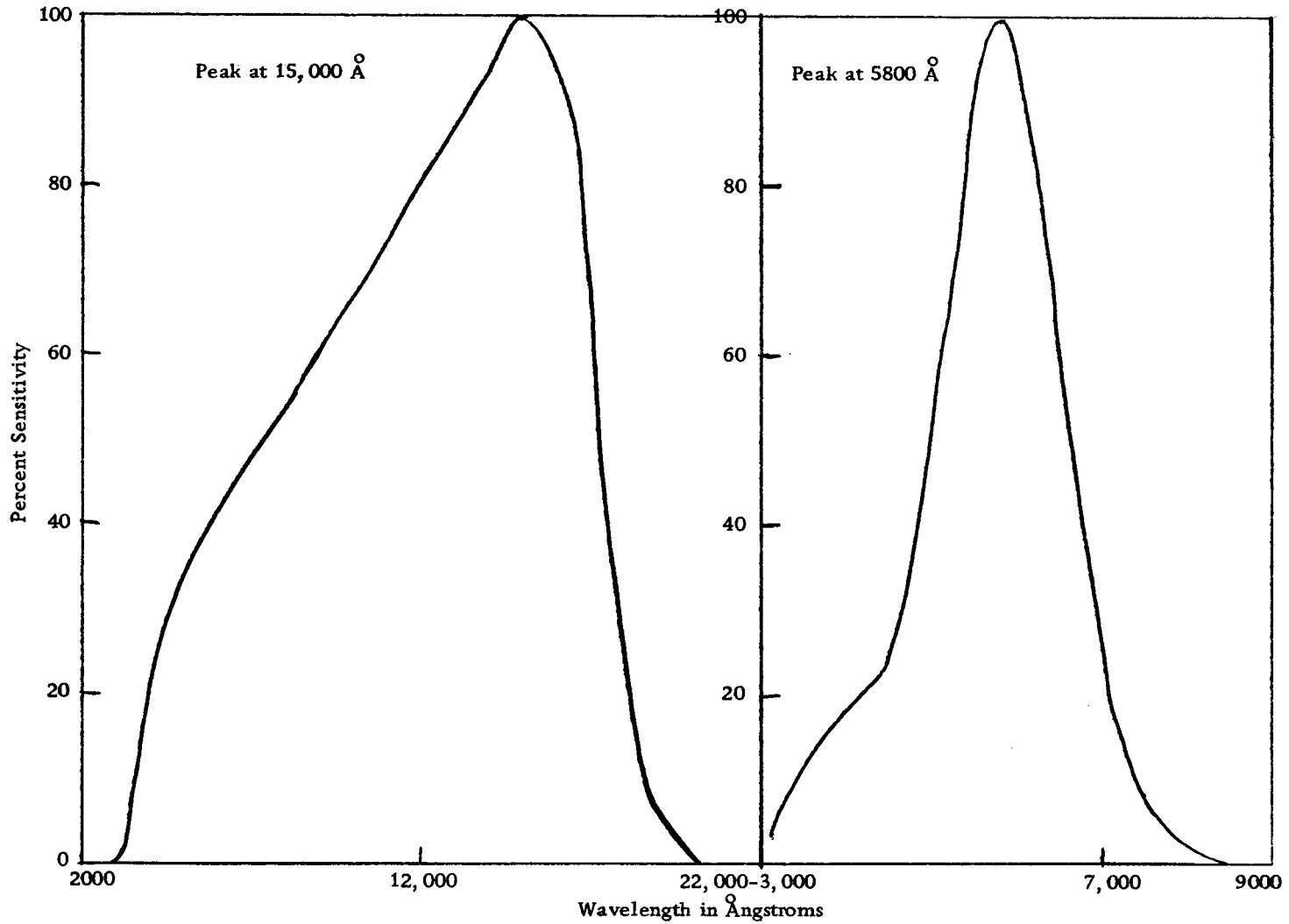


FIGURE 18. RCA S-14 Photoconductor Cell (26).

FIGURE 19. RCA S-15 Photoconductor Cell (26).

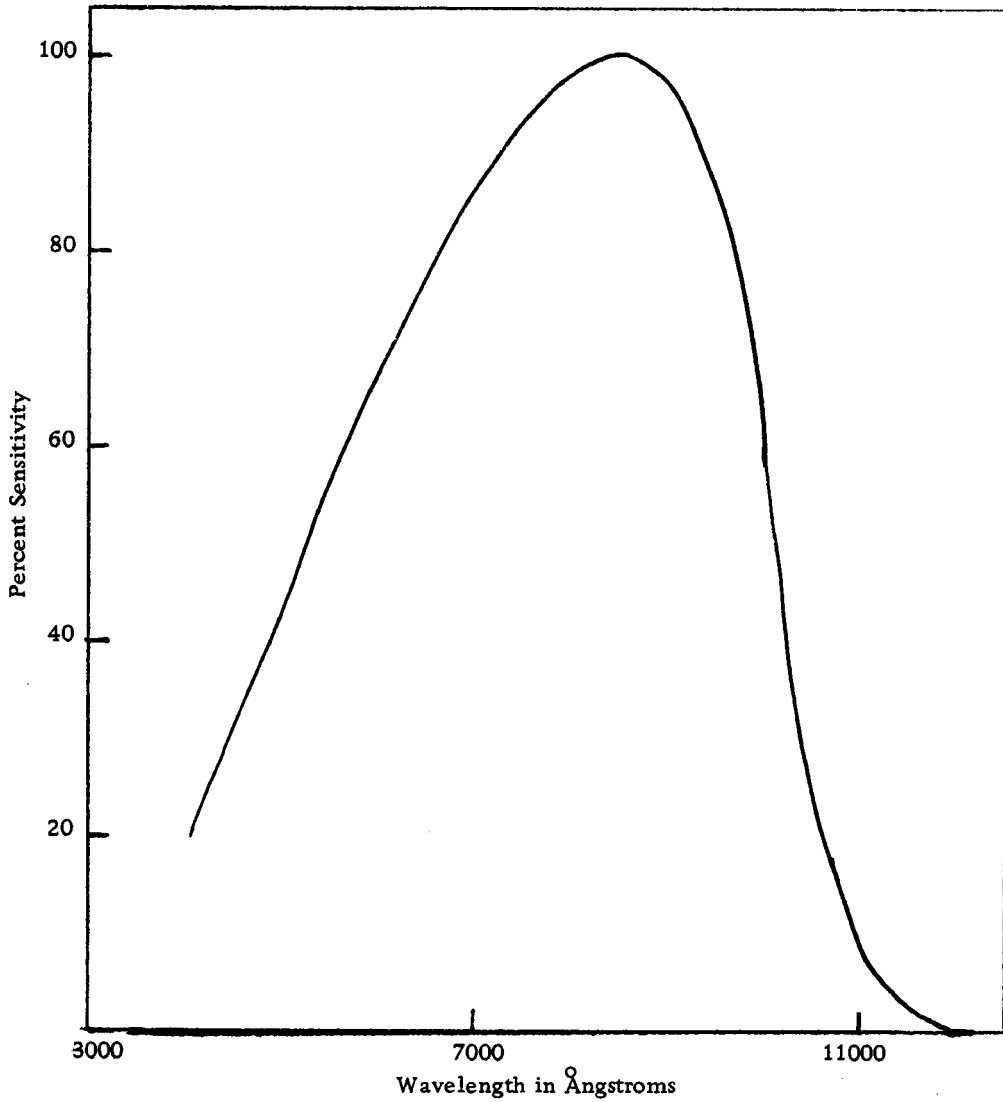


FIGURE 20. RCA Photovoltaic Cell Spectral Absorbion Characteristics For Cell Types SL 2205 and SL 2206 (26).

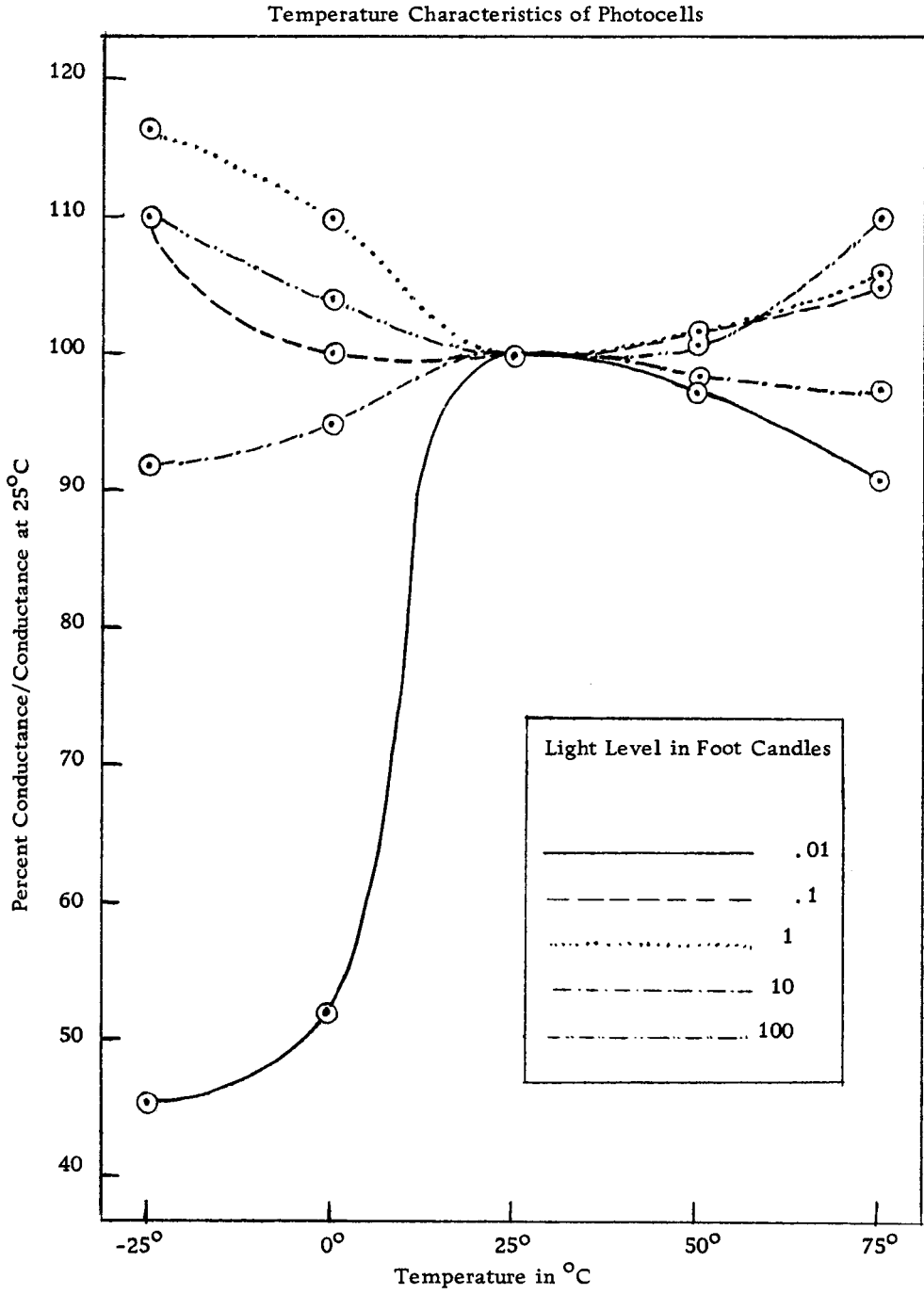


FIGURE 21. Clairex Type 2 Photoconductor Cell Cadmium Sulfide (2).

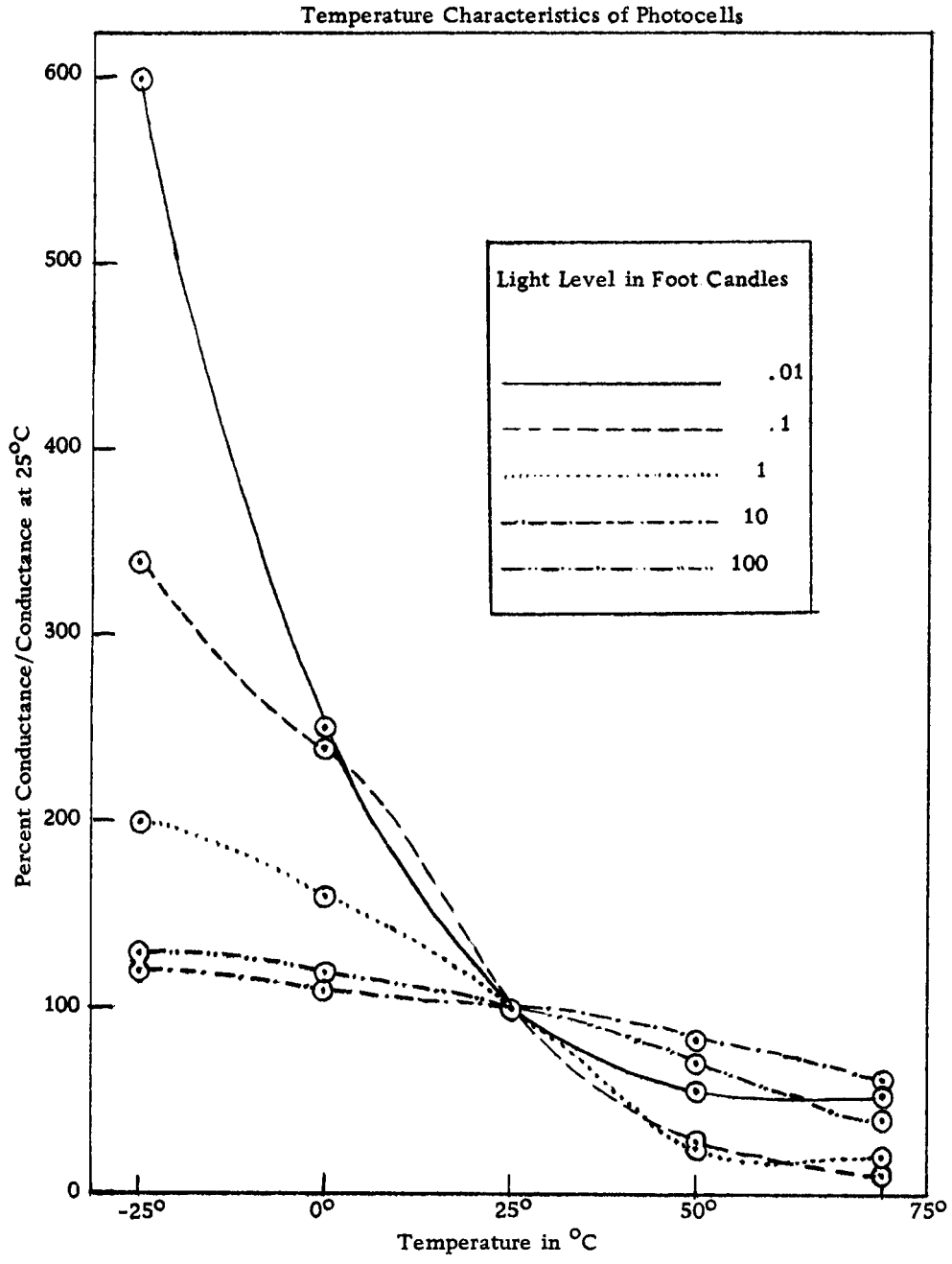


FIGURE 22. Clairex Type 3 Photoconductor Cell Cadmium Selenide (2).

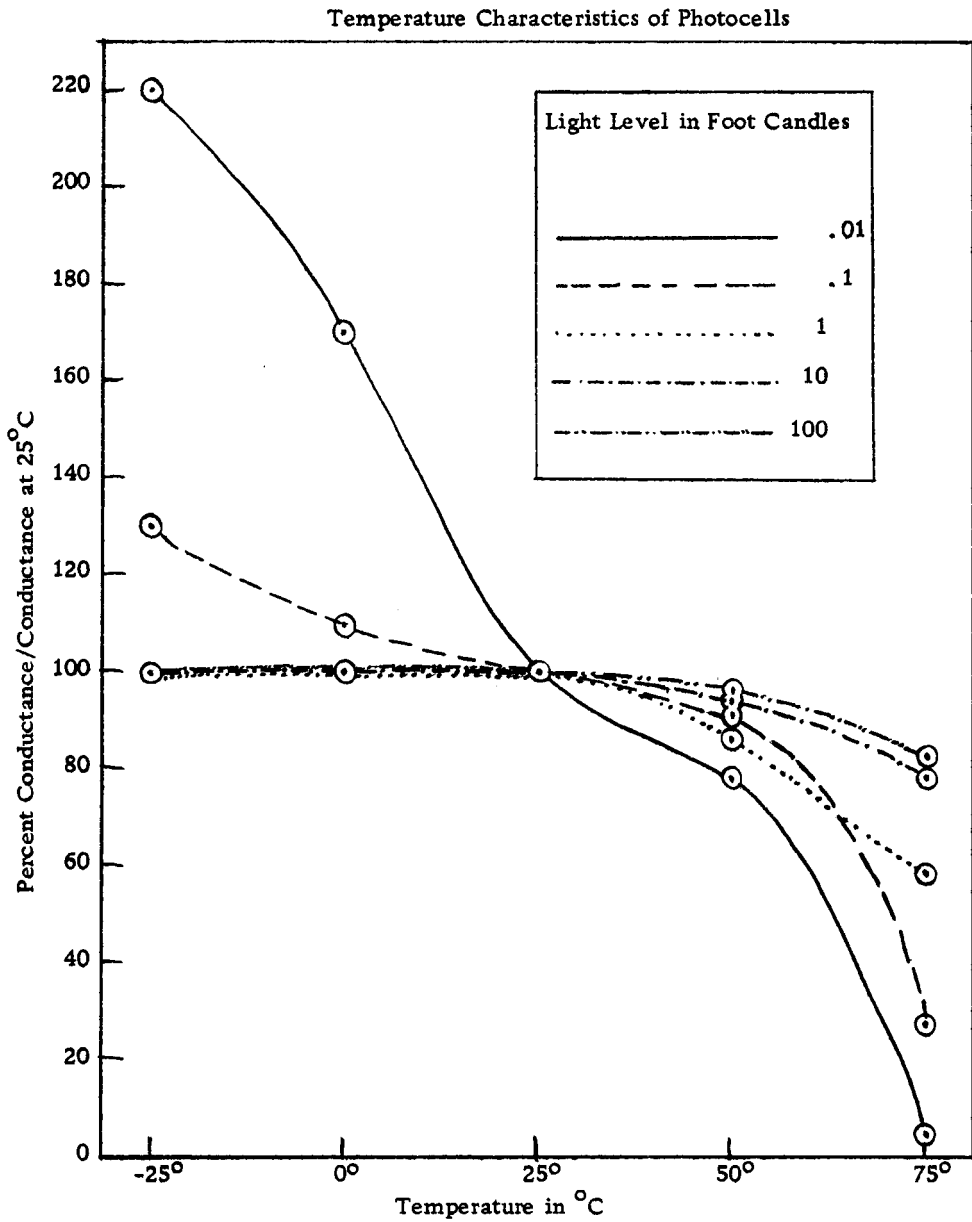


FIGURE 23. Clairex Type 4 Photoconductor Cell Cadmium Selenide (2).

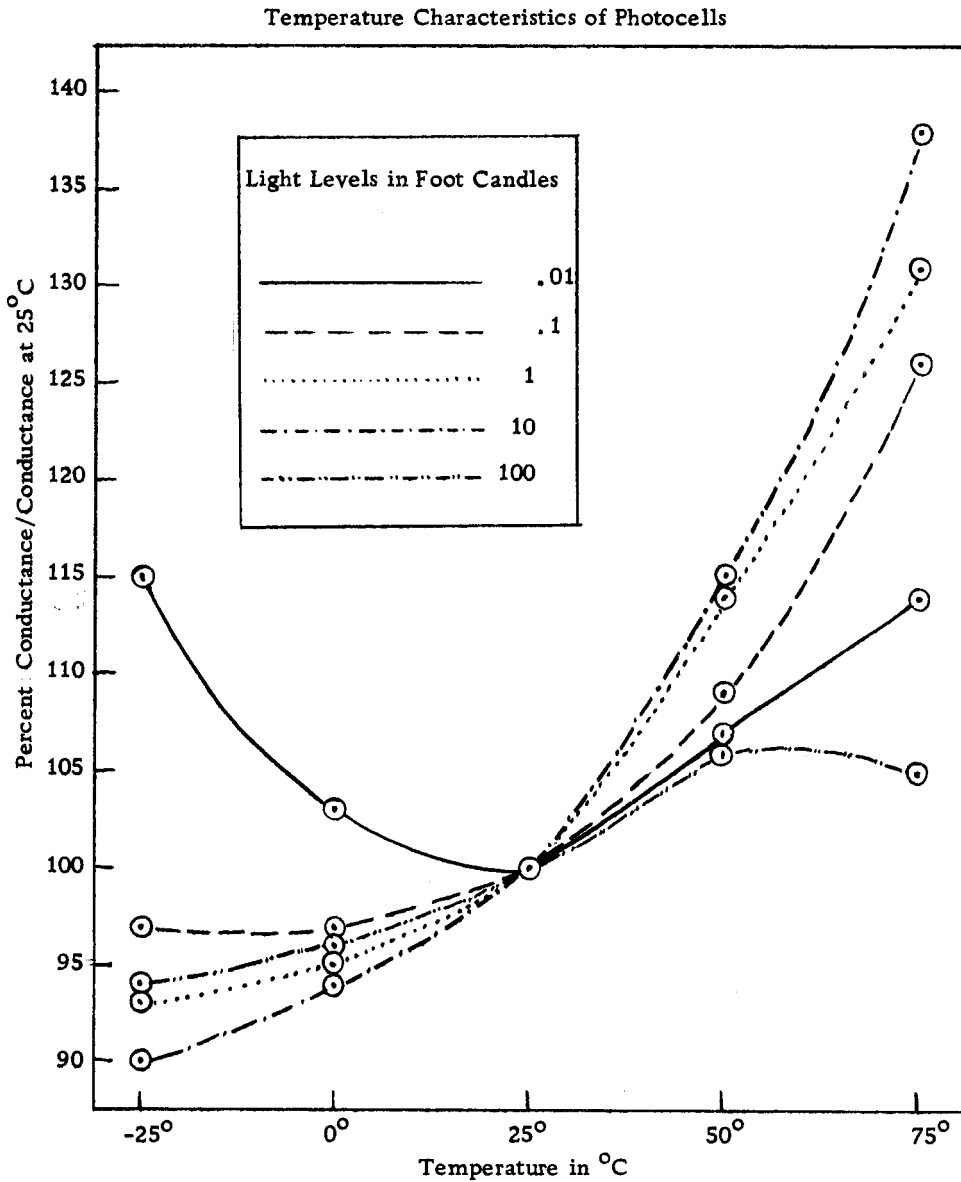


FIGURE 24. Clairex Type 5 Photoconductor Cell Cadmium Sulfide (2).

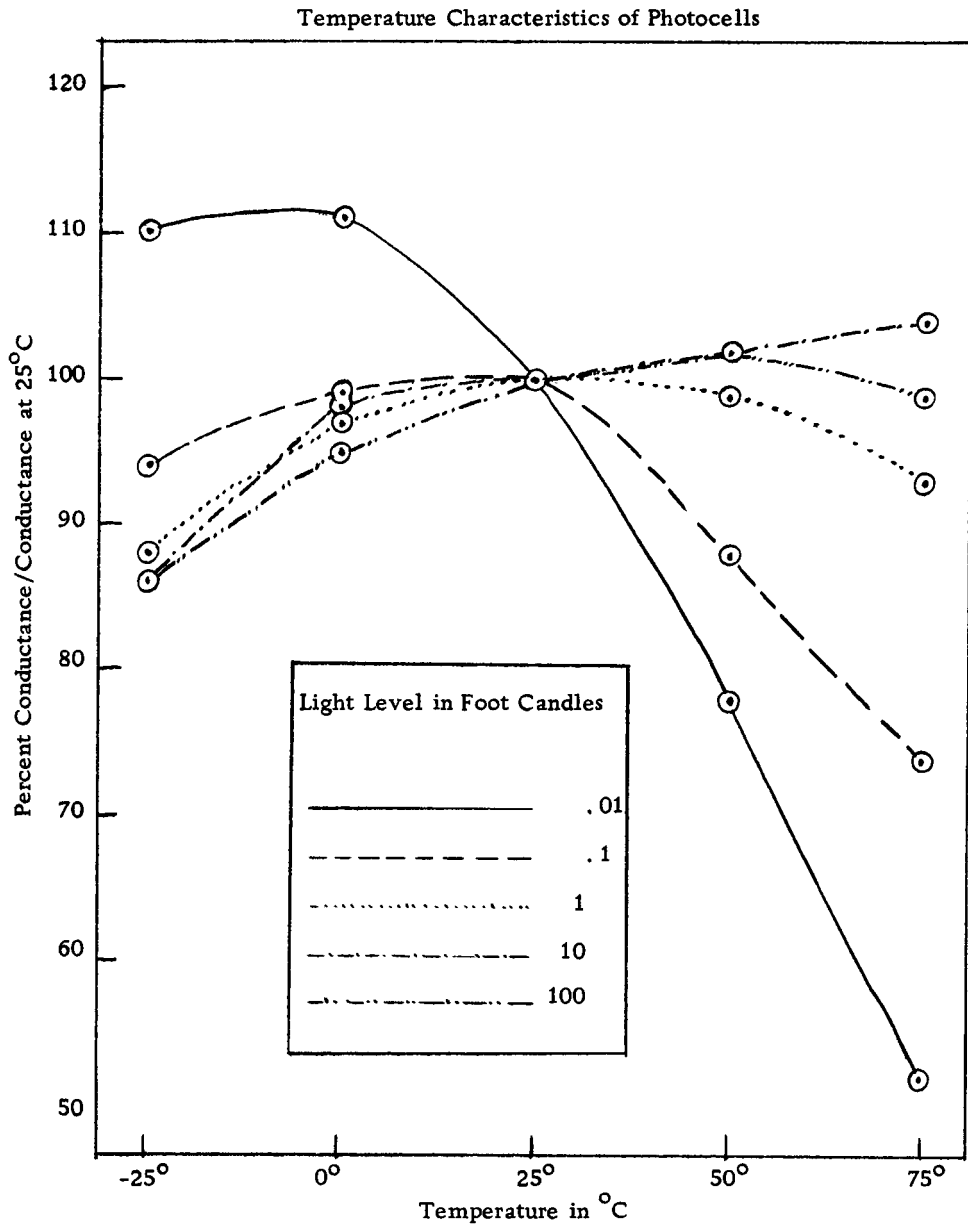


FIGURE 25. Clairex Type 7 Photoconductor Cell Cadmium Sulfide (2).

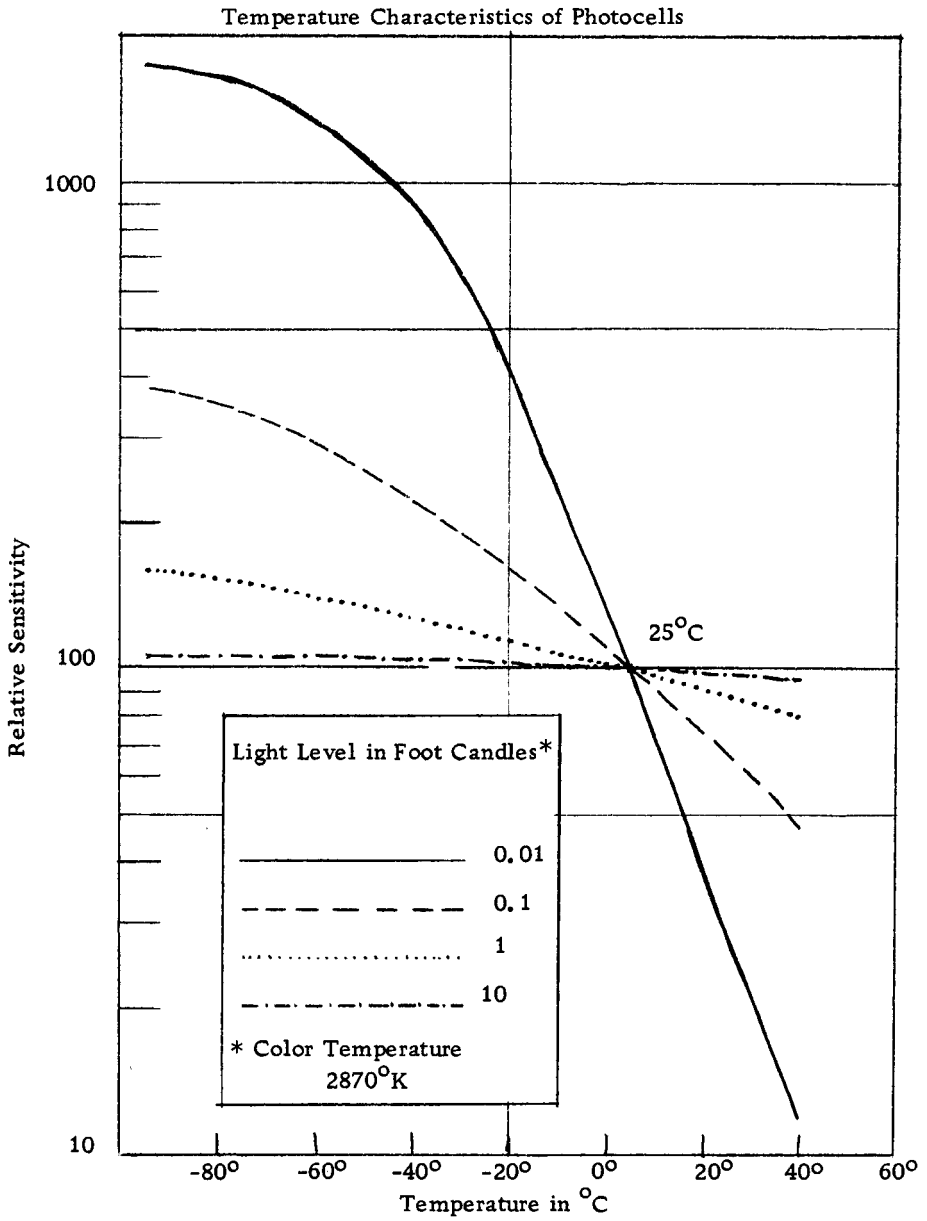


FIGURE 26. Typical Temperature Characteristics of an RCA Cadmium Sulfide Photoconductor Cell (26).

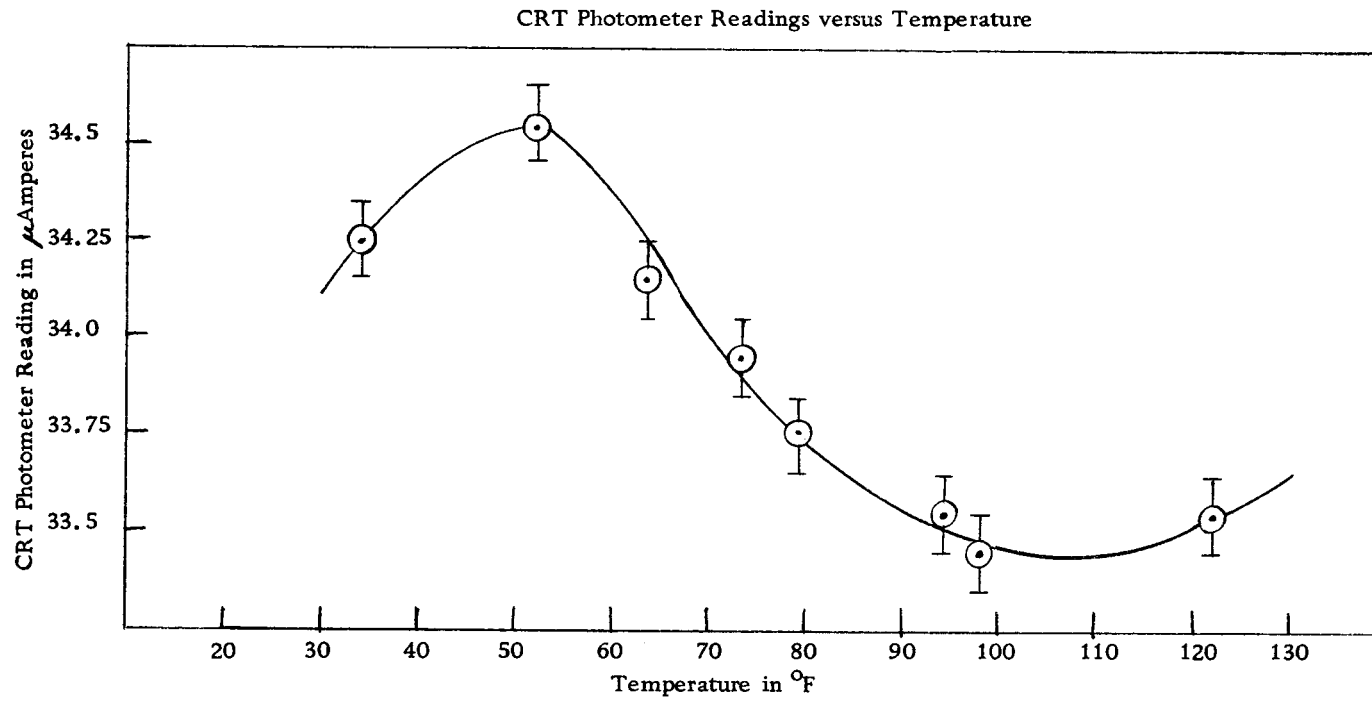


FIGURE 27. CRT Photometer Readings versus Temperature

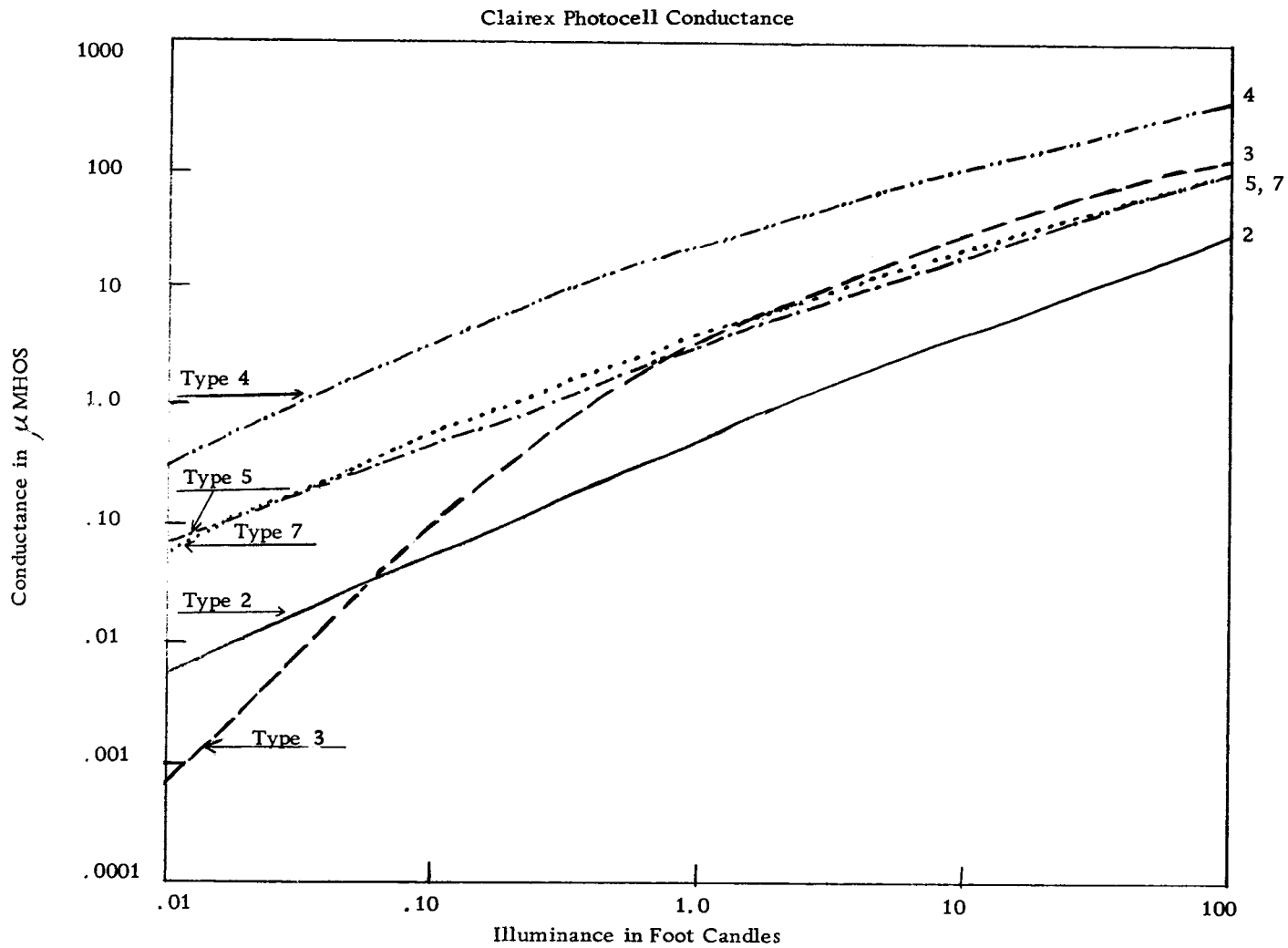


FIGURE 28. Clairex Photocell Conductance (2).